

AD-A054 726

SYSTEMS EXPLORATION INC SAN DIEGO CA

F/6 17/2

HF CHANNEL SIMULATOR FOR WIDEBAND SIGNALS. A MATHEMATICAL MODEL--ETC(U)

MAR 78 R LUGANNANI, H C BOOKER, L E HOFF

N00123-76-C-1090

UNCLASSIFIED

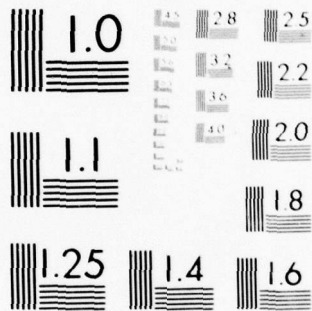
NOSC-TR-20A

ALL

1 OF 2  
AD  
A054726

NOSC





MICROCOPY RESOLUTION TEST CHART  
NATIONAL BUREAU OF STANDARDS-1963-A



FOR FURTHER TRAN

12

AD A 054726

NOSC

# NOSC

NOSC TR 208

Technical Report 208

## HF CHANNEL SIMULATOR FOR WIDEBAND SIGNALS

A Mathematical Model and Computer Program for  
100-kHz Bandwidth HF Channels

R Lugannani and HG Booker  
LE Hoff (Contract Monitor)  
31 March 1978

Final Report: February 1977 - October 1977

Prepared for  
Naval Electronic Systems Command

APPROVED FOR PUBLIC RELEASE; DISTRIBUTION UNLIMITED

NAVAL OCEAN SYSTEMS CENTER  
SAN DIEGO, CALIFORNIA 92152

DDC  
RECEIVED  
JUN 8 1978  
B

AD No. \_\_\_\_\_  
DDC FILE COPY



NAVAL OCEAN SYSTEMS CENTER, SAN DIEGO, CA 92152

---

AN ACTIVITY OF THE NAVAL MATERIAL COMMAND

RR GAVAZZI, CAPT, USN

Commander

HL BLOOD

Technical Director

ADMINISTRATIVE INFORMATION

Work was performed under contract N000123-76-C-1090/SEI-C-020 by Systems Exploration, Inc. for Intra-Task Force/SS Com Branch, Communications Systems and Technology Department, NOSC.

This work was performed as part of NAVELEX's Skywave Communications Task, a 6.2 Block-Funded Program. This report covers work from February 1977 to October 1977 and was approved for publication January 1978.

Released by  
CA NELSON, Head  
Surface/Shore Systems Division

Under authority of  
RO EASTMAN, Head  
Communications Systems and  
Technology Department

UNCLASSIFIED

SECURITY CLASSIFICATION OF THIS PAGE (When Data Entered)

19 REPORT DOCUMENTATION PAGE		READ INSTRUCTIONS BEFORE COMPLETING FORM
1. REPORT NUMBER 18 NOSCTR-298	2. GOVT ACCESSION NO.	3. RECIPIENT'S CATALOG NUMBER
4. TITLE (and Subtitle) 6 HF Channel Simulator for Wideband Signals. A Mathematical Model and Computer Program for 100-kHz Bandwidth HF Channels.	5. TYPE OF REPORT & PERIOD COVERED 9 Final Report February 1977 - October 1977	6. PERFORMING ORG. REPORT NUMBER
7. AUTHOR(s) 10 R. LUGANNANI, HC BOOKER LE Hoff (Contract Monitor)	8. CONTRACT OR GRANT NUMBER(s) 15 N000123-76-C-1090 SEI-C-020	9. PROGRAM ELEMENT, PROJECT, TASK AREA & WORK UNIT NUMBERS 16 62721N; E21222 17 XF21222091 (B194)
9. PERFORMING ORGANIZATION NAME AND ADDRESS Systems Exploration, Inc. 3687 Voltaire St. San Diego, CA 92106	11. CONTROLLING OFFICE NAME AND ADDRESS Naval Electronic Systems Command Code 3105 Washington, DC 20360	12. REPORT DATE 11 31 March 1978
14. MONITORING AGENCY NAME & ADDRESS (if different from Controlling Office) NAVAL OCEAN SYSTEMS CENTER San Diego, CA 92152 12 103 p.	15. SECURITY CLASS. (of this report) UNCLASSIFIED	13. NUMBER OF PAGES
16. DISTRIBUTION STATEMENT (of this Report) Approved for public release; distribution unlimited.		
17. DISTRIBUTION STATEMENT (of the abstract entered in Block 20, if different from Report)		
18. SUPPLEMENTARY NOTES		
19. KEY WORDS (Continue on reverse side if necessary and identify by block number) High frequency      FORTRAN Simulators      Broadband Broadband Model      Channels		
20. ABSTRACT (Continue on reverse side if necessary and identify by block number) A simulator has been developed that is capable of modeling the wideband HF channel. It is designed for carrier frequencies in the 2-32 MHz range and it can accommodate bandwidths up to 100 kHz and ground ranges up to 1000 km. It models the groundwave and ionosphere returns, but does not include additive noise or signal distortion produced in the transmitter or receiver. The inputs are the basic physical quantities that characterize the ionosphere (height, thickness, and maximum electron density of the E and F regions, sunspot number, time of day, etc) and those quantities that characterize the transmitter-receiver environment (carrier frequency, range, geographic location, antenna patterns, etc). Explicit values for channel parameters such as delay, attenuation, and doppler		

DD FORM 1473  
1 JAN 73EDITION OF 1 NOV 65 IS OBSOLETE  
S/N 0102-LF 014-6601

UNCLASSIFIED

SECURITY CLASSIFICATION OF THIS PAGE (When Data Entered)

31c 115  
403972

1/5

UNCLASSIFIED

SECURITY CLASSIFICATION OF THIS PAGE(When Data Entered)

20. shift and spread are not required as these are calculated internally.

The simulator is divided into two parts. The first part is concerned with the mathematical model of the ionosphere and the computation of the channel parameters from the basic inputs. These channel parameters are used in the second part to determine the response for arbitrary inputs. A software version of the simulator has been implemented and tested, and a Fortran listing of the program is appended. The program runs in non-real time and requires a computer with a Fortran IV compiler and at least 28 K of core.

ACCESSION	
NTIS	<input checked="" type="checkbox"/> YES <input type="checkbox"/> NO
DOC	<input type="checkbox"/> YES <input type="checkbox"/> NO
UNCLASSIFIED	<input type="checkbox"/> YES <input type="checkbox"/> NO
JUSTIFICATION	
BY	
DISTRIBUTION/AVAILABILITY CODES	
Dist.	AVAIL. and/or SPECIAL
A	

UNCLASSIFIED

SECURITY CLASSIFICATION OF THIS PAGE(When Data Entered)



## OBJECTIVE

Develop a mathematical model for the wideband HF channel and the software implementation of this model. The model must be valid for carrier frequencies in the 2-32 MHz range, for bandwidths up to 100 kHz, and for ground ranges up to 1000 km.

## RESULTS

A simplified model of the ionosphere is employed to determine the various skywave returns and the effect these returns have on the overall received signal. The groundwave is modeled as a delayed, attenuated version of the transmitted signal. Inputs to the simulator consist of those basic physical quantities that characterize the ionosphere and those that characterize the transmitter-receiver environment; values of delay, attenuation, doppler shift and spread, and dispersion are calculated internally for each component of the received signal. A FORTRAN version of the simulator has been written and tested for several typical channels.

## RECOMMENDATIONS

Make further refinements in the mathematical model in order to expand the scope and accuracy of the simulator. Of particular value in this regard would be the inclusion of a deviative absorption term for the skywave returns and the inclusion of an attenuation term for propagation of the groundwave over a rough, lossy ocean surface.

Investigate the relationship between the simulator inputs and the actual observed returns as measured, for example, by an ionosonde. A knowledge of this relationship would provide further verification of the mathematical model as well as a set of inputs that correspond to known operating conditions.

Finally, in view of the meager data base available in the wideband case, any measurement program aimed at enlarging this data base would represent a significant contribution to the study and modeling of HF channels.

## GLOSSARY

### English Letter Symbols

$a$	Multiplicative constant used to generate random sequence $\{Y_n\}$
$a_j(n)$	Impulse response of filter used to generate approximate random gain $G_j(nT_o)$
$A$	Multiplicative constant for doppler shift
$A_g$	Gain of groundwave
$A_j$	RMS gain of $j$ -th ionosphere path
$A(x)$	$= 2 G \tan \theta$
$B$	Multiplicative constant for doppler spread
$B_r$	Bearing of receiver as seen from transmitter in magnetic coordinates
$BW$	Two-sided bandwidth of transmitted signal
$c$	Velocity of light
$C_{G_j}(\tau)$	Correlation function of $G_j(t)$
$C_{G_j}^\lambda(\tau)$	Correlation function of $G_j^\lambda(t)$
$C_{U_j}(\tau)$	Correlation function of $U_j^{(1)}(t)$ and $U_j^{(2)}(t)$
$D$	Virtual path length
$D_g$	Delay of groundwave
$D_j^{(o)}$	$= f_c \cdot \tau_j^{(o)}$
$D_j^{(k)}$	$= \frac{1}{k!} [k\tau_j^{(k-1)} + f_c \tau_j^{(k)}], k = 1, 2, \dots$
$f$	Frequency
$f_c$	Carrier frequency

# GLOSSARY (Continued)

$f_r$	Doppler reference frequency
$f_{HD}$	Gyrofrequency of D region
$f_{HE}$	Gyrofrequency of E region
$f_{HF}$	Gyrofrequency of F region
$f_{pE}$	General expression for penetration frequency of E region (ordinary or extraordinary wave)
$f_{pF}$	General expression for penetration frequency of F region (ordinary or extraordinary wave)
$f_{pE}^{(o)}$	Penetration frequency of E region - ordinary wave
$f_{pE}^{(x)}$	Penetration frequency of E region - extraordinary wave
$f_{pF}^{(o)}$	Penetration frequency of F region - ordinary wave
$f_{pF}^{(x)}$	Penetration frequency of F region - extraordinary wave
$G = G(f)$	Group height of signal path, oblique incidence
$G_j(t)$	Random gain of j-th path
$\tilde{G}_j(t)$	Approximation for random gain of j-th path
$G_R(\theta)$	Gain of receiving antenna
$G_T(\theta)$	Gain of transmitting antenna
$G_v = G_v(f)$	Group height of signal path, vertical incidence
$h$	Height above earth
$h_D$	Height of peak electron density of D region
$h_E$	Height of peak electron density of E region

# GLOSSARY (Continued)

$h_F$	Height of peak electron density of F region
$h_r$	Height at which refractive index equals zero at vertical incidence
$h_j(t)$	Distortion impulse response of j-th path
$\hat{h}_j(t)$	Modified distortion impulse response: $=T_o h_j(t)$
$2H_E$	Semithickness of E region electron density
$2H_F$	Semithickness of F region electron density
$H_j(f)$	Fourier transform of $h_j(t)$
$I$	Angle of inclination of earth's magnetic field
$I(x)$	Cannonical expression representing general impulse response $\hat{h}_j(t)$
$I_p(x)$	Integrals used in series representation of $I(x)$
$k$	Sunspot number multiplier for non-deviative absorption loss
$K$	Multiplicative constant for non-deviative absorption loss
$K_j$	Constant used in the generation of $\hat{G}_j(nT_o)$
$L_{abs}$	Absorption loss
$L_{ant}$	Antenna pattern loss
$L_d$	Spreading loss
$L_j$	Total loss of j-th path
$M$	Length of pseudo random sequence
$N=N(h)$	Electron density
$N_E$	Maximum electron density of E region



# GLOSSARY (Continued)

$N_F$	Maximum electron density of F region
$N_g$	Integer multiple of $T_0$ nearest the groundwave delay $D_g$
$N_j$	Integer multiple of $T_0$ nearest the signal delay $D_j$
$P_{G_j}(f)$	Power spectral density of $G_j(t)$
$P_{\tilde{G}_j}(f)$	Power spectral density of $\tilde{G}_j(t)$
$P_{U_j}(f)$	Power spectral density of $U_j^{(1)}(t)$ and $U_j^{(2)}(t)$
$r(t)$	Received, complex, baseband signal
$R$	Distance between transmitter and receiver
$s(t)$	Transmitted, complex, baseband signal
$\tilde{s}_j(t)$	Distorted, complex signal returned from ionosphere via j-th path
$\hat{s}_j(t)$	Distorted, complex signal returned from ionosphere via j-th path after removal of phase and delay components: $\tilde{s}_j(t) = \exp[-2\pi i D_j^{(0)}] \hat{s}_j(t - D_j^{(1)})$
$S$	Sunspot number
$S(f)$	Fourier transform of $s(t)$
$t$	Time
$T_0$	Sampling interval (one half the Nyquist interval of the transmitted signal)
$u_1, u_2$	Uniform [0,1] random variables
$U_j^{(1)}(t), U_j^{(2)}(t)$	Real, independent, zero mean identically-distributed, Gaussian process used to define $G_j(t)$
$W_j(1), W_j(2), W_j(3)$	Independent, complex, Gaussian random variables used in generation of $G_j(nT_0)$
$x$	$= \cos \theta$
$\{Y_n\}$	Sequence of pseudo random integers

## GLOSSARY (Continued)

### Greek Letter Symbols

$\alpha$	Doppler shift exponent
$\beta$	Doppler spread exponent
$\gamma$	Exponent of solar zenith angle term in expression for nondeviative absorption
$\gamma_j(1), \gamma_j(2)$	Constants used in the generation of $\tilde{G}_j(nT_o)$
$\Delta^{(2)}$	General amplitude distortion coefficient
$\Delta^{(3)}$	General phase distortion coefficient
$\Delta_j^{(2)}$	Normalized amplitude distortion coefficient of j-th path
$\Delta_j^{(3)}$	Normalized phase distortion coefficient of j-th path
$\eta$	Normalized frequency variable = $f/BW$
$\theta$	Ray angle of signal path measured from vertical
$\kappa$	$= (e^2/4\pi^2\epsilon_o m) \approx 80.5$
$\lambda$	Geographic longitude
$\lambda_o$	Geographic longitude of north magnetic pole
$\lambda_j(1), \lambda_j(2)$	Constants used in the generation of $\tilde{G}_j(nT_o)$
$\mu$	Refractive index
$\nu$	General doppler shift
$\nu_j$	Doppler shift of j-th path
$\nu_r$	Reference doppler shift

# GLOSSARY (Continued)

$\xi$	Complex Gaussian random variable
$\xi_j(n)$	Independent, identically-distributed Gaussian sequence
$\xi_j^{(1)}(n)$	Real part of $\xi_j(n)$
$\xi_j^{(2)}(n)$	Imaginary part of $\xi_j(n)$
$\rho$	Parameter used in fitting $C_{G_j}(\tau)$ to $C_{G_j}(\tau)$
$2\sigma$	General doppler spread
$2\sigma_j$	Doppler spread of j-th path
$2\sigma_r$	Reference doppler spread
$\tau$	General path delay
$\tau_j(f)$	Delay of j-th path as a function of frequency
$\tau_j^{(k)}$	k-th derivative of delay of j-th path evaluated at the carrier frequency $f_c$
$\phi$	Geographic latitude
$\phi_o$	Geographic latitude of north magnetic pole
$\Phi$	Magnetic latitude
$\chi$	Solar zenith angle
$\psi_i$	Angle between earth's magnetic field and wave incident upon ionosphere
$\psi_r$	Angle between earth's magnetic field and wave reflected from ionosphere

## TABLE OF CONTENTS

<u>Section</u>	<u>Page</u>
I. INTRODUCTION. . . . .	1
II. THE HF CHANNEL . . . . .	3
III. MATHEMATICAL MODEL OF THE IONOSPHERE. . . . .	10
A. Delay and Delay Derivatives . . . . .	10
B. Attenuation . . . . .	17
B.1 Absorption. . . . .	17
B.2 Antenna Gain . . . . .	19
B.3 Spreading Loss . . . . .	19
C. Doppler. . . . .	20
D. Computer Program. . . . .	22
IV. SIGNAL ANALYSIS. . . . .	29
A. Delay Distortion. . . . .	30
B. Random Gains . . . . .	33
C. Computer Program. . . . .	34
V. CONCLUDING REMARKS. . . . .	36
VI. REFERENCES . . . . .	38
Appendix A - Delay and Delay Derivatives. . . . .	A-1
Appendix B - Program for Calculating Channel Parameters . . . . .	B-1
Appendix C - Computer Generation of Random Gains. . . . .	C-1
Appendix D - Signal Analysis Program . . . . .	D-1



## LIST OF FIGURES

<u>Figure</u>	<u>Page</u>
1    Block Diagram of Simulator. . . . .	9
2    Virtual and Actual Signal Paths . . . . .	10
3    Nighttime Electron Density Profile . . . . .	13
4    Daytime Electron Density Profile. . . . .	14
5    Computed Ionosphere Returns for One, Two and Three Hops. . . . .	28
6    Normalized Correlation Function for the Random Gains. . . . .	35

## LIST OF TABLES

<u>Table</u>	<u>Page</u>
1    Default Values for Doppler Shift and Doppler Spread . . . . .	22
2    Typical Output Listing for Computed Channel Parameters . . . . .	23
3    Index Convention for Ionosphere Returns . . . . .	25
4    Glossary of Terms used for Computed Channel Parameters . . . . .	26
5    Typical Output Listing for Computed Channel Parameters (Includes only those Returns Having Attenuations within 40 dB of the Smallest Nonzero Attenuation) . . . .	27

## I. INTRODUCTION

The use of channel simulators to study the performance of communication systems and to assist in their design has become increasingly popular in recent years. By employing a simulator, it is possible to reproduce given channel characteristics as desired and to compare different system designs in identical environments. Moreover, the cost of simulation is usually much less than the cost of "on the air" measurements and it is quite reliable. A variety of HF channel simulators have been proposed and studied in the past [1-4]\*. Sailors and Hill [5] have written an excellent survey of the field and have made several recommendations for future work. Some of these recommendations are embodied in the present report.

In the following the development of a simulator for the wide-band HF channel is described. This simulator is designed for carrier frequencies in the 2-32 MHz range and it can accommodate bandwidths up to 100 kHz and ground ranges up to 1000 km. The simulator models the groundwave and all ionosphere returns (both single and multiple hops), but does not include additive noise or signal distortion produced in the transmitter or receiver. It takes into account all ionospheric phenomena that have a significant effect on wideband communications. Many of these phenomena, such as delay differences between the ordinary and extraordinary waves and signal distortion caused by variations of delay with frequency, have been neglected in the earlier simulators, resulting in severe bandwidth limitations. The inputs required are the basic parameters that characterize the physical ionosphere (height, thickness, and maximum electron density of the E and F regions, sunspot number, time of day, etc.) and those that characterize the transmitter and receiver (carrier frequency, range, geographic location, antenna patterns, etc.). Since these input parameters are the ones that are actually known in practice it is a simple matter to vary them and observe the effect they have on system performance. This

---

\*References are listed in Section VI.

capability does not exist in the previous simulators which require as inputs not the basic quantities mentioned above but those channel parameters such as delay, attenuation, doppler shift and doppler spread derived from them.

In the course of developing the simulator a number of simplifications and approximations have been made to obtain tractable results. The most important of these assumptions concerns the electron density profile and the absorption mechanism. It is recognized that the ionosphere model used does not provide a detailed physical characterization of the ionosphere; however, it does provide an "order of magnitude" characterization suitable for communication purposes. The simulator is divided into two parts. The first part is concerned with the mathematical model of the ionosphere and the computation of the channel parameters from the basic inputs. The second part uses these parameters to determine the channel response for arbitrary inputs. Both parts of the simulator are described in detail in the following sections.

## II. THE HF CHANNEL

The signal received via the HF channels considered in this report is the sum of the groundwave and the various ionosphere returns. Throughout we shall assume that the groundwave is an attenuated, delayed version of the transmitted signal but is otherwise undistorted. The ionosphere returns also suffer attenuation and delay but in addition are subject to fading and distortion. There is also time dispersion (multipath) produced by the different delays associated with each ionosphere return. The purpose of this section is to present some definitions that are used in the sequel and to introduce the mathematical model for the HF channel.

The complex transmitted baseband signal will be denoted by  $s(t)$  and its Fourier transform by  $S(f)$ . Thus

$$s(t) = \int_{-\infty}^{\infty} S(f) \exp [2\pi i f t] df. \quad (1)$$

Distorted versions of this signal will be returned from the ionosphere for both the E region and the F region (low ray and high ray). There will be a set of these returns for the ordinary and extraordinary magnetoionic components and for as many multiple-hop paths as are present. Although many returns are possible, all but a few of these experience a large attenuation and the number of effective returns is usually small. In the following we will denote the number of effective ionosphere returns by  $N$ . This number is determined by excluding all returns that suffer an attenuation greater than some predetermined value.

Distortion of signals reflected from the ionosphere has been studied by several authors, who have attempted to characterize the impulse response for a simplified model of the ionosphere [6-10]. Unfortunately, these results have been derived using ionosphere



models that are too idealized for our purposes<sup>1</sup> and the impulse responses obtained are too complicated for easy implementation<sup>2</sup>. In order to obtain tractable expressions for the distortion we shall assume that it is caused primarily by the fact that the delay is a function of frequency and is not constant across the signal bandwidth. This characterization of the distortion mechanism allows us to make a number of approximations which result in relatively simple expressions for the distorted signal. For obvious reasons we shall refer to this particular distortion as delay distortion.

Let  $f_c$  denote the carrier frequency and let  $\tau_j(f)$  denote the delay of the  $j$ -th return as a function of frequency. It follows from (1) that the distorted baseband signal returned from the ionosphere is given by

$$\tilde{s}_j(t) = \int_{-\infty}^{\infty} S(f) \exp [-2\pi i(f_c+f) \cdot \tau_j(f_c+f)] \cdot \exp [2\pi i f t] df. \quad (2)$$

$j = 1, \dots, N$

We will characterize this distortion by the coefficients in the power series expansion of the delay about the carrier frequency. This series appears as

$$\tau_j(f_c+f) = \sum_{k=0}^{\infty} \frac{f^k}{k!} \tau_j^{(k)}, \quad j=1, \dots, N \quad (3)$$

---

<sup>1</sup>They allow for reflection only from a single ionospheric region and consider such simple electron density profiles as a constant and a linear function of height.

<sup>2</sup>In one case the impulse response is given as the solution of an integral equation.

with

$$\tau_j^{(k)} = \frac{d^k}{df^k} \tau_j(f_c + f) \Big|_{f=0} . \quad (4)$$

Substituting this series into the exponential delay term in (2) we obtain

$$\exp[-2\pi i(f_c + f) \cdot \tau_j(f_c + f)] = \exp \left[ -2\pi i \sum_{k=0}^{\infty} f^k D_j^{(k)} \right] \quad (5)$$

$j=1, \dots, N$

where we have defined

$$D_j^{(0)} = f_c \tau_j^{(0)} \quad j=1, \dots, N \quad (6)$$

and

$$D_j^{(k)} = \frac{1}{k!} \left[ k \tau_j^{(k-1)} + f_c \tau_j^{(k)} \right] \quad \begin{matrix} k=1, 2, \dots \\ j=1, \dots, N. \end{matrix} \quad (7)$$

Thus, for  $\tilde{s}_j(t)$  we have

$$\begin{aligned} \tilde{s}_j(t) = & \exp[-2\pi i D_j^{(0)}] \int_{-\infty}^{\infty} s(f) \exp \left[ -2\pi i \sum_{k=2}^{\infty} f^k D_j^{(k)} \right] \\ & \cdot \exp[2\pi i f(t - D_j^{(1)})] df. \end{aligned} \quad (8)$$

$j=1, \dots, N$

For computational reasons it is convenient to separate the phase and delay terms from the actual distortion of the signal. To this end we define a function  $\hat{s}_j(t)$  as follows

$$\tilde{s}_j(t) = \exp[-2\pi i D_j^{(0)}] \hat{s}_j(t - D_j^{(1)}) \quad (9)$$

$j=1, \dots, N$

where

$$\hat{s}_j(t) = \int_{-\infty}^{\infty} S(f) H_j(f) \exp[2\pi i f t] df, \quad j=1, \dots, N \quad (10)$$

with

$$H_j(f) = \exp\left[-2\pi i \sum_{k=2}^{\infty} f^k D_j^{(k)}\right], \quad j=1, \dots, N. \quad (11)$$

In practice it is convenient to determine  $\hat{s}_j(t)$  by performing a time domain convolution rather than by evaluating the Fourier transform (10). If the impulse response determined by  $H_j(f)$  is denoted by  $h_j(t)$ , we have

$$h_j(t) = \int_{-\infty}^{\infty} H_j(f) \exp[2\pi i f t] df, \quad j=1, \dots, N., \quad (12)$$

and the desired convolution appears as

$$\hat{s}_j(t) = \int_{-\infty}^{\infty} s(t-u) h_j(u) du, \quad j=1, \dots, N. \quad (13)$$

A discussion of the approximations used in the numerical evaluation of  $h_j(t)$  and  $\hat{s}_j(t)$  is presented in Section IV.

In addition to the above distortion, the ionosphere returns are subject to attenuation and random fading. These two phenomena are included by multiplying the delayed, distorted signal by a random gain, which we denote by  $G_j(t)$ . We will assume that  $G_j(t)$  is a complex, zero-mean, Gaussian process with identically-distributed real and imaginary parts. This is the Rayleigh fading model [11]. While the assumption of Rician fading [12] would provide somewhat more flexibility than the Rayleigh assumption, the available evidence [12-14] indicates that the Rayleigh model is adequate for our purposes. The random gains associated with different returns are assumed to be independent.

Let  $U_j^{(1)}(t)$  and  $U_j^{(2)}(t)$  denote two real, independent zero mean, identically-distributed, stationary Gaussian processes with correlation function

$$C_{U_j}(\tau) = E U_j^{(1)}(t+\tau) U_j^{(1)}(t) = E U_j^{(2)}(t+\tau) U_j^{(2)}(t). \quad (14)$$

$$j=1, \dots, N.$$

The corresponding power spectral density is given by

$$P_{U_j}(f) = \int_{-\infty}^{\infty} C_{U_j}(\tau) \exp[-2\pi i f \tau] d\tau, j=1, \dots, N. \quad (15)$$

We define the random gain in terms of  $U_j^{(1)}(t)$  and  $U_j^{(2)}(t)$  as follows

$$G_j(t) = [U_j^{(1)}(t) + i U_j^{(2)}(t)] \cdot \exp[2\pi i v_j t] \quad (16)$$

$$j=1, \dots, N.$$

where  $v_j$  is the doppler shift for the  $j$ -th ionosphere return. The correlation and power spectral density of  $G_j(t)$  are easily determined using the assumed properties of  $U_j^{(1)}$  and  $U_j^{(2)}(t)$ . Thus

$$C_{G_j}(\tau) = E G_j(t+\tau) G_j^*(t) = 2C_{U_j}(\tau) \cdot \exp[2\pi i v_j \tau] \quad (17)$$

$$j=1, \dots, N.$$

and

$$P_{G_j}(f) = 2P_{U_j}(f-v_j), j=1, \dots, N. \quad (18)$$

Following Watterson [1] we assume that the power spectral density  $P_{G_j}(f)$  has a Gaussian shape. While there is no conclusive experimental evidence for this assumption, it is a convenient model for spectra that are unimodal and that decrease rapidly. Specifically we let



$$c_{G_j}(\tau) = A_j^2 \exp[-2\pi^2 \sigma_j^2 \tau^2 + 2\pi i v_j \tau] \quad . \quad (19)$$

$j=1, \dots, N$

Here  $A_j$  is the rms gain ( $0 \leq A_j \leq 1$ ) of the  $j$ -th return and  $2\sigma_j$  is the doppler spread of the return. The power spectral density associated with this correlation function is

$$P_{G_j}(f) = \frac{A_j^2}{\sqrt{2\pi} \sigma_j} \exp \left[ -\frac{(f-v_j)^2}{2\sigma_j^2} \right] \quad , \quad j=1, \dots, N. \quad (20)$$

Finally, we must add the groundwave to the ionosphere returns. The groundwave is assumed to experience only delay and to have a non-random gain. If  $A_g$  denotes the gain ( $0 \leq A_g \leq 1$ ) and  $D_g$  denotes the delay, the contribution to the received signal from the groundwave is given by  $A_g s(t-D_g)$ . The gain is a complicated function of range, sea state and frequency. Graphs of this functional relationship are given in [15].

Summarizing the above, the complex, baseband received signal can be expressed as

$$r(t) = A_g s(t-D_g) + \sum_{j=1}^N \exp[-2\pi i D_j^{(0)}] G_j(t) \hat{s}_j(t-D_j^{(1)}) \quad . \quad (21)$$

A block diagram illustrating (21) is presented in Figure 1.

In the following sections, the quantities needed in the evaluation of  $r(t)$  are derived and the techniques employed in its numerical evaluation are described.

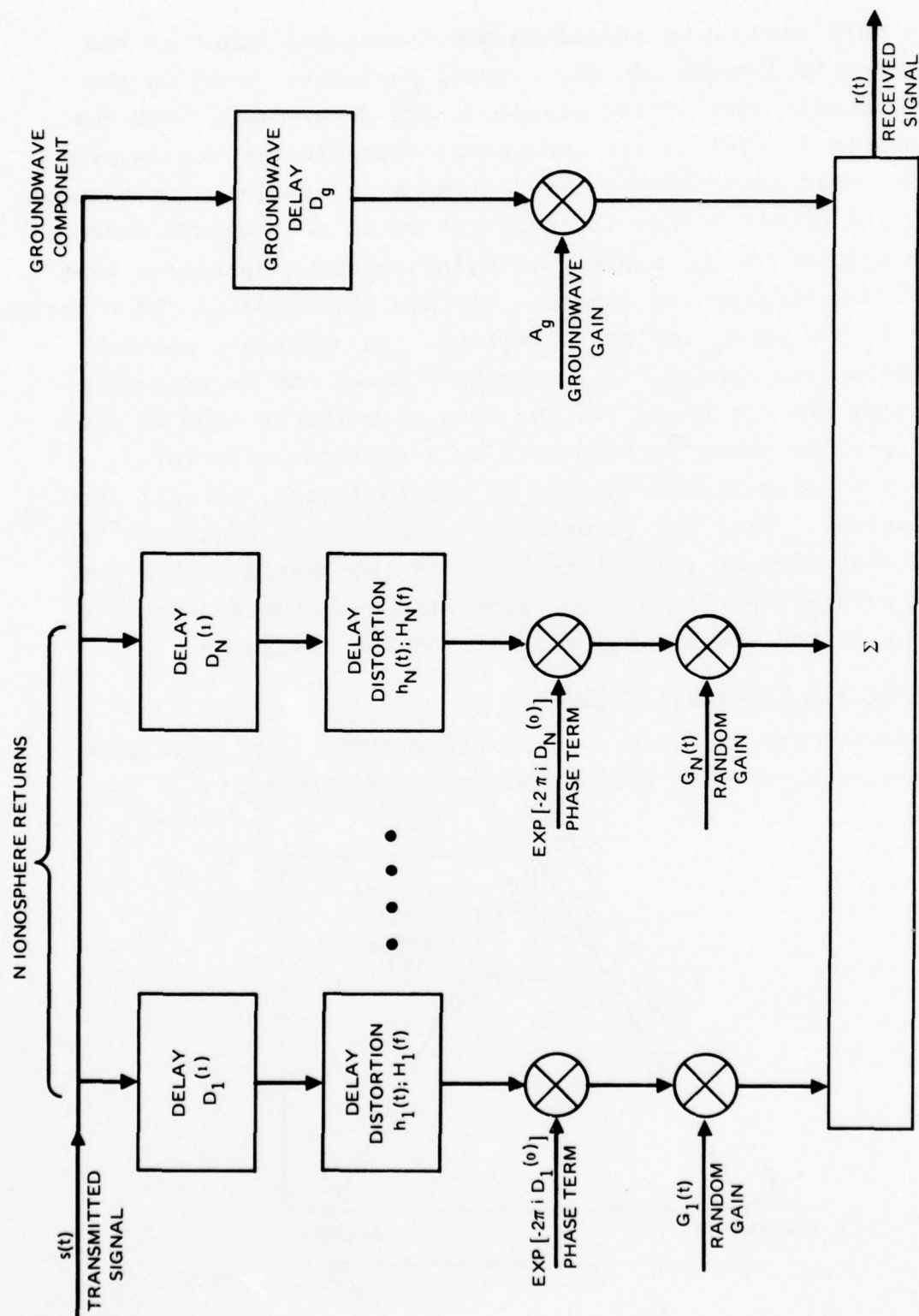


Figure 1. Block Diagram of Simulator

### III. MATHEMATICAL MODEL OF THE IONOSPHERE

In this section we introduce a mathematical model of the ionosphere and discuss how the channel parameters used in the signal analysis part of the simulator are determined. Our goal is to obtain a model of the ionosphere suitable for use in mid-latitude ocean environments. Differences in transmission between daytime and nighttime are included but we do not include those effects related to the rapidly changing electron densities that occur during sunrise and sunset. Daytime splitting of the F region into an  $F_1$  and an  $F_2$  region is omitted. In addition, neither transmission via sporadic E or spread F modes nor M- or N-type reflections are included. In the case of multiple hops we will assume that the ocean surface acts as a perfect reflector.

As a notational convenience in the following, we will drop the subscript  $j$  from all quantities. However, it should be kept in mind that each of these quantities is associated with a particular return, and it must be identified with the appropriate subscript in the signal analysis part of the simulator.

#### A. Delay and Delay Derivatives

To determine the group delay of the signal reflected from the ionosphere, we make use of the following figure.

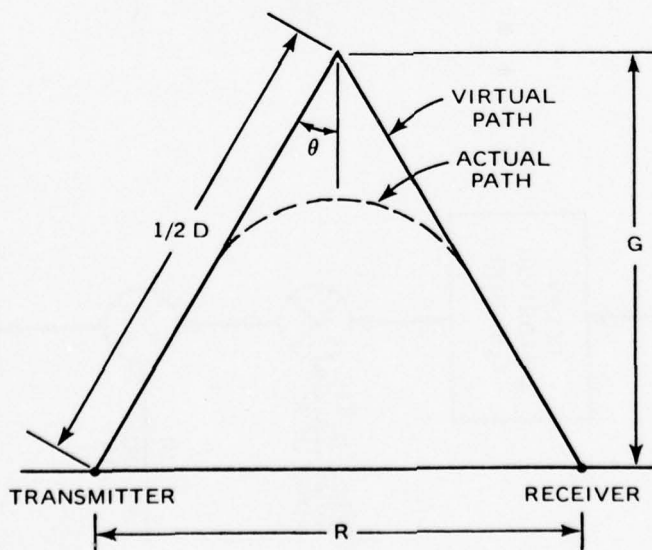


Figure 2. Virtual and Actual Signal Paths

Here the dashed line is the actual ionospheric path of the signal between the transmitter and the receiver and the solid line is the virtual path. The ground range between transmitter and receiver is denoted by  $R$ , the virtual path length by  $D$ , the ray angle measured from the vertical by  $\theta$  and the group height by  $G$ . Assuming a flat earth and ionosphere, we have by simple geometry

$$D = \frac{R}{\sin \theta} = \frac{R}{(1-x^2)^{1/2}} \quad (22)$$

where we have defined  $x = \cos \theta$ . If  $c$  denotes the velocity of light, the signal delay is given by the virtual path length divided by  $c$

$$\tau = \frac{R}{c(1-x^2)^{1/2}} \quad (23)$$

It remains to determine the ray angle  $\theta$ .

For vertical incidence ( $\theta=0$ ), the group height is given by the integral [16]

$$G_V = G_V(f) = \int_0^{h_r} \frac{dh}{\mu} \quad (24)$$

where  $\mu$  is the refractive index and  $h_r$  is the height at which  $\mu=0$ . In the absence of both collisions and the earth's magnetic field, the refractive index is given by [16]

$$\mu^2 = (1 - \kappa \frac{N}{f^2}) \quad (25)$$

where  $N = N(h)$  is the electron density in  $m^{-3}$ ,  $f$  is the frequency in Hz and  $\kappa = (e^2/4\pi^2\epsilon_0 m) \approx 80.5$ . The group height for oblique incidence is the same as for vertical incidence but we must replace  $f$  by  $f \cos \theta$  [16]. That is  $G = G(f) = G_V(f \cos \theta)$ . Once the group height has been determined, we appeal to Figure 2 to obtain the relationship

$$R = 2 G \tan \theta = 2 G \left( \frac{1-x^2}{x^2} \right)^{1/2} \quad (26)$$



Defining

$$A(x) = 2 G \left( \frac{1-x^2}{2} \right)^{1/2} \quad (27)$$

we see that, for a specified range  $R$ , we must solve the transcendental equation

$$R = A(x) \quad (28)$$

for  $x$  and then substitute this into (23) to obtain the delay.

We seek an approximation to the electron density for which the group height,  $G$ , can be expressed in a simple closed form. Our main concern here is with reflections from the E and F regions. At nighttime we assume that the electron density profile can be represented by two distinct parabolas as shown in Figure 3. Let  $N_E$  be the peak electron density of the E region in  $m^{-3}$ , let  $h_E$  be the height of the peak electron density of the E region in km, and let  $2H_E$  be the semithickness of the E region in km; similar definitions are made for the F region. Then the nighttime electron density is given by

$$N(h) = \begin{cases} 0 & h < h_E - 2H_E \\ N_E \left[ 1 - \left( \frac{h - h_E}{2H_E} \right)^2 \right] & h_E - 2H_E < h < h_E + 2H_E \\ 0 & h_E + 2H_E < h < h_F - 2H_F \\ N_F \left[ 1 - \left( \frac{h - h_F}{2H_F} \right)^2 \right] & h_F - 2H_F < h < h_F + 2H_F \\ 0 & h_F + 2H_F < h \end{cases} \quad (29)$$

In the daytime the electron density profile is also assumed to be parabolic but allowance is made for ionization between the E and F regions. The electron density between the two regions is assumed to be constant and equal to the peak value of the E region. This is illustrated in Figure 4. Using the same definitions as before, the daytime electron density is given by

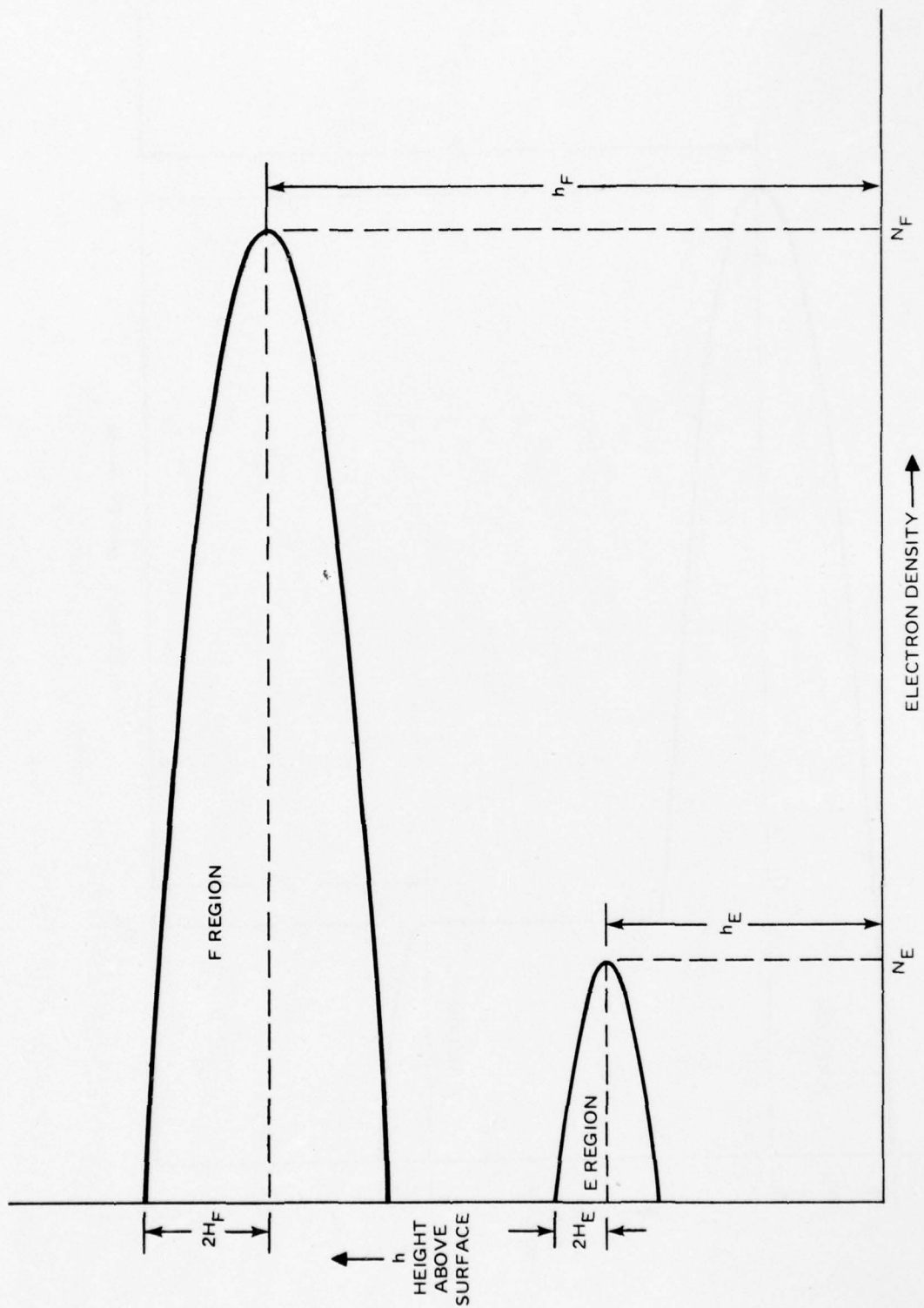


Figure 3. Nighttime Electron Density Profile

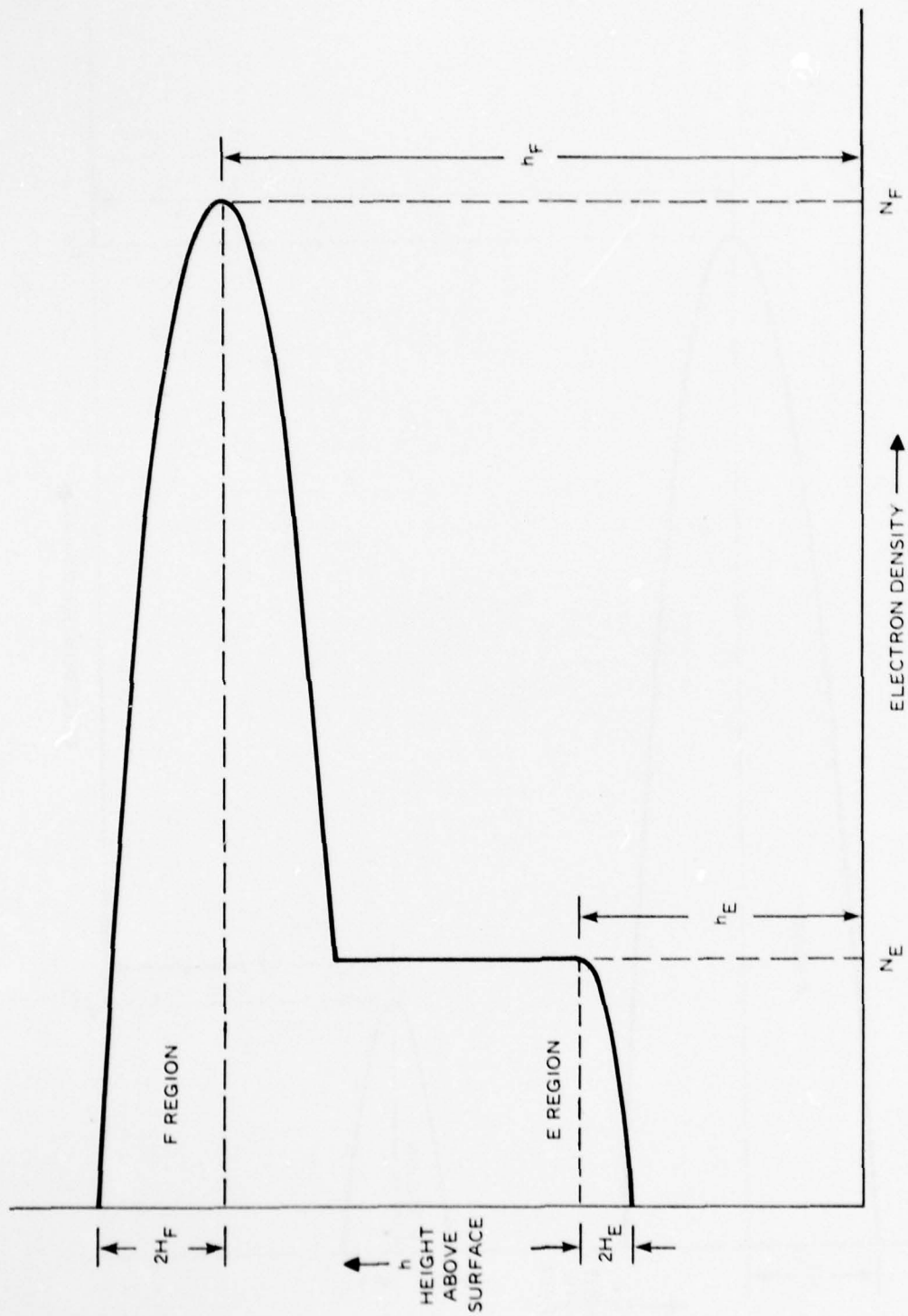


Figure 4. Daytime Electron Density Profile

$$N(h) = \begin{cases} 0, & h < h_E - 2H_E \\ N_E \left[ 1 - \left( \frac{h - h_E}{2H_E} \right)^2 \right], & h - 2H_E < h < h_E \\ N_E, & h_E < h < h_F + 2H_F \left( 1 - \frac{N_E}{N_F} \right)^{\frac{1}{2}} \\ N_F \left[ 1 - \left( \frac{h - h_F}{2H_F} \right)^2 \right], & h_F + 2H_F \left( 1 - \frac{N_E}{N_F} \right)^{\frac{1}{2}} < h < h_F + 2H_F \\ 0, & h_F + 2H_F < h. \end{cases} \quad (30)$$

Note that the constants appearing in (24) and (30) will be different owing to the different heights and ionization densities for nighttime and daytime conditions.

A quantity of interest in the present analysis is the penetration frequency of each region. This is defined as the plasma frequency at the peak electron density [16]. We have for the E and F regions

$$f_{pE}^2 = \kappa N_E \quad (31a)$$

$$f_{pF}^2 = \kappa N_F \quad (31b)$$

where  $\kappa = (e / 4\pi \epsilon_0 m)^2 \approx 80.5$  and the two penetration frequencies are in Hz. The physical interpretation of  $f_{pE}$  and  $f_{pF}$  is that they represent the maximum frequencies at which signals will be reflected from the respective regions at vertical incidence.

Returning to the determination of the group height,  $G$ , it is a relatively simple matter to evaluate the integral (24) for either of the above electron densities [17]. The details of this evaluation are presented in Appendix A.

In the foregoing the effect of the earth's magnetic field has been neglected, but we take this to be an adequate approximation for the ordinary wave. For the extraordinary wave, however, the penetration frequencies are shifted relative to those for the ordinary wave, and it is essential to take this into account.

Denoting the penetration frequencies of the ordinary and extraordinary waves by the superscripts "o" and "x" we have [16]

$$f_{pE}^{(x)} = \frac{1}{2} f_{HE} + \left[ f_{HE}^2 + 4 (f_{pE}^{(o)})^2 \right]^{\frac{1}{2}} \quad (32a)$$

$$f_{pF}^{(x)} = \frac{1}{2} f_{HF} + \left[ f_{HF}^2 + 4 (f_{pF}^{(o)})^2 \right]^{\frac{1}{2}} \quad (32b)$$

Here  $f_{pE}^{(o)}$  and  $f_{pF}^{(o)}$  are defined by (31), and  $f_{HE}$  and  $f_{HF}$  are the gyrofrequencies associated with the earth's magnetic field at the levels of maximum ionization density in the E and F regions. For the gyrofrequencies in mHz we will use the approximate expressions [16]

$$f_{HE} = 0.87 \left( \frac{6370}{6370 + h_E} \right)^3 (1 + 3 \sin^2 \phi)^{\frac{1}{2}} \quad (33a)$$

$$f_{HF} = 0.87 \left( \frac{6370}{6370 + h_F} \right)^3 (1 + 3 \sin^2 \phi)^{\frac{1}{2}} \quad (33b)$$

where  $\phi$  is the latitude expressed in magnetic coordinates. If  $\phi$  and  $\lambda$  are respectively the geographic latitude and longitude, and  $\phi_0$  and  $\lambda_0$  represent the latitude and longitude of the north magnetic pole ( $\phi_0 \approx 78.3^\circ N$ ,  $\lambda_0 \approx 69^\circ W$ ), then [16]

$$\sin \phi = \sin \phi \sin \phi_0 + \cos \phi \cos \phi_0 \cos (\lambda - \lambda_0) \quad (34)$$

We assume that, to calculate delays for the extraordinary wave, we may use the expressions in Appendix A but with  $f_{pE}^{(x)}$  and  $f_{pF}^{(x)}$  substituted for the ordinary wave penetration frequencies. Otherwise the calculations of delay are assumed to take the same form as those for the ordinary wave.



To characterize delay distortion we need the derivatives of the delay evaluated at the carrier frequency. Actually, only the first three derivatives are required for the approximation discussed in Section IV. The determination of these three derivatives is straightforward although the resulting expressions are quite complicated. They are listed in Appendix A.

For multiple hop transmissions we assume that the ionosphere parameters are identical for each hop. In the two-hop case the foregoing analysis is applied with the original range multiplied by 1/2. The angle is then correct as calculated but the path length, delay and delay derivatives must be multiplied by 2. Higher numbers of hops are treated in a similar manner using appropriate multipliers.

## B. Attenuation

Three main sources of attenuation are included in the present model. They are: (1) nondeviative absorption, (2) antenna gain, and (3) spreading ( $1/r^2$  loss). Other factors such as focusing and polarization mismatch will also affect the received signal strength, but these are assumed to be of secondary importance and they have accordingly been omitted.

### B.1 Absorption

Absorption is assumed to take place only in the D region of the ionosphere and only in the daytime. The absorption is assumed to be nondeviative, i.e., it takes place in a region where the refractive index is near unity. The attenuation will be characterized by the expression [16]

$$L_{\text{abs}} = K \sec \theta \cdot (1+kS) \cdot (\cos \chi)^\gamma \quad (35)$$

$$\cdot \left\{ \frac{1}{(f \pm f_{\text{HD}} |\cos \psi_i|)^2} + \frac{1}{(f \pm f_{\text{HD}} |\cos \psi_r|)^2} \right\}.$$

Here  $L_{\text{abs}}$  is the attenuation due to absorption in decibels per hop,  $\theta$  is the ray angle measured from the vertical,  $S$  is the sunspot number,  $\chi$  is the solar zenith angle,  $f$  is the frequency in MHz,  $f_{\text{HD}}$  is the gyrofrequency at the D region level in MHz and  $\psi_i$  [resp.,  $\psi_r$ ] is the angle between the earth's magnetic field and the incident [resp., reflected] wave. The plus sign is used for the ordinary wave and the minus sign is used for the extraordinary wave.

The relative importance of the sunspot number and solar zenith angle depends upon the constants  $K$ ,  $k$  and  $\gamma$ ; following Davies [16, p. 235] we will set  $K = 215$ ,  $k = 0.0035$  and  $\gamma = 0.75$ . The gyrofrequency,  $f_{\text{HD}}$ , is given by [16]

$$f_{\text{HD}} = 0.87 \left( \frac{6370}{6370+h_D} \right)^3 (1+3 \sin^2 \phi)^{\frac{1}{2}} \quad (36)$$

where  $h_D$  is the height of the D region in km and  $\phi$  is the latitude in magnetic coordinates. In this expression we will take  $h_D$  to be 70 km and use (34) to determine  $\sin \phi$ . The angles  $\psi_i$  and  $\psi_r$  are determined from the relationships

$$\cos \psi_i = \sin \theta \cos B_r \cos I + \cos \theta \sin I \quad (37a)$$

$$\cos \psi_r = \sin \theta \cos B_r \cos I - \cos \theta \sin I \quad (37b)$$

where  $B_r$  is the bearing of the receiver as seen from the transmitter in magnetic coordinates and  $I$ , the angle of inclination of the earth's magnetic field, is given by

$$\tan I = -2 \tan \phi. \quad (38)$$

For multiple-hop paths, the expression (35) must be multiplied by the number of hops.

## B.2 Antenna Gain

No attempt has been made in this model to provide a variety of antenna patterns. While any desired antenna gain can be easily included in the program, we shall use the gain of a short vertical dipole for both transmitter and receiver. If  $G_T$  and  $G_R$  denote the transmitter and receiver power gains relative to isotropic antennas we have

$$G_T(\theta) = G_R(\theta) = \frac{3}{2} \sin^2 \theta. \quad (39)$$

Thus for the overall attenuation in decibels we have

$$L_{\text{ant}} = -10 \log_{10} G_T(\theta) - 10 \log_{10} G_R(\theta) = -20 \log_{10} \left[ \frac{3}{2} \sin^2 \theta \right]. \quad (40)$$

## B.3 Spreading Loss

The decrease in signal strength attributable to the length of the transmission path is given by

$$L_d = 20 \log_{10} \left( \frac{4\pi Df}{0.3} \right) \quad (41)$$

where  $L_d$  is the path loss in decibels,  $D$  is the total path length in km, taking into account any multiple hops, and  $f$  is the frequency in MHz.

The total attenuation for a particular ionosphere return is obtained by adding (35), (40) and (41), after making any necessary adjustments for multiple hops. Denoting the total attenuation for the  $j$ -th return by  $L_j$  we have

$$L_j = L_{\text{abs}} \times (\text{No. of Hops}) + L_{\text{ant}} + L_d. \quad (42)$$



The rms gain  $A_j$  is thus given by

$$A_j = 10^{-(L_j/20)} . \quad (43)$$

### C. Doppler

The remaining quantities needed to characterize the random gains,  $G_j(t)$ , are the doppler shifts and the doppler spreads. In this report we are not concerned with the relatively large doppler values that occur during sunrise and sunset, but with the smaller values that are typical of the ionosphere for the majority of a typical twenty-four hour period. What is desired is the shift and spread associated with each of the propagation modes. Unfortunately, measurements that have been made concerning doppler values usually have not been concerned with the shift and spread of the individual propagation modes; instead they have recorded composite doppler values involving many modes [18]. Moreover, most theoretical studies have not been concerned with communication system performance and are of marginal value for present purposes [19-22].

What is required for our model is an expression relating the doppler shifts and spreads to frequency for each ionosphere return. This expression will depend on the electron density profile and its time rate of change as well as on various other ionosphere parameters [23]. We assume that the doppler values can be characterized adequately by the following power laws

$$\nu = A f^\alpha \quad (44)$$

and

$$\sigma = B f^\beta \quad (45)$$

where  $\nu$  and  $2\sigma$  are the doppler shift and doppler spread;  $f$  is the frequency in mHz; and  $A$ ,  $B$ ,  $\alpha$ , and  $\beta$  are constants that characterize the region from which the wave is reflected and the magnetoionic

component involved. In general we need an expression of the above type for the low and high ray returns from each region and for each magnetoionic component.

It is convenient to express the constants A and B appearing in (44) and (45) in terms of a reference value measured at a known frequency. Thus the above expressions can be rewritten as

$$\nu = \nu_r (f/f_r)^\alpha \quad (46)$$

$$\sigma = \sigma_r (f/f_r)^\beta \quad (47)$$

where  $\nu_r$  and  $2\sigma_r$  are the doppler shift and spread measured at the reference frequency  $f_r$ . For multiple hops we assume that the doppler effects combine incoherently so that

$$\nu = (\text{No. of Hops}) \cdot \nu_r \cdot (f/f_r)^\alpha \quad (48)$$

and

$$\sigma = (\text{No. of Hops})^{1/2} \cdot \sigma_r \cdot (f/f_r)^\beta \quad (49)$$

Given the appropriate reference values and exponents, the above expressions provide the doppler shift and spread for each ionosphere return. However, since the reference values and exponents usually are not known, we must make some assumptions to obtain "default" values for use in the absence of more accurate data. It will be assumed that the doppler shift and spread are the same for the high ray and low ray and for both magnetoionic components of the E and F region returns. The following table gives the "default" reference values and exponents to be used for the E and F regions. These values are based upon measurements made by Watterson, et. al. [1].

Region	$\nu_r$ (Hz)	$2\sigma_r$ (Hz)	$f_r$ (mHz)	$\alpha$	$\beta$
E	0.01	0.02	9.30	1.0	1.0
F	0.01	0.15	9.30	1.0	1.0

Table 1. Default Values for Doppler Shift and Doppler Spread

#### D. Computer Program

The Fortran program used to calculate the foregoing channel parameters is presented in Appendix B. The basic output of this program is a listing of the input parameters and a tabular presentation of the computed channel parameters. A typical output is shown in Table 2. The indexing convention used for the returns is presented in Table 3 and a glossary of the terms used in the output is presented in Table 4.

A modified version of this output can be produced in which all returns whose attenuation exceeds some threshold value above the minimum attenuation are omitted. Those modes for which there is no return are likewise omitted. Using this modified output one can identify those returns that are of primary interest for communication purposes. An example is shown in Table 5 using the same inputs that produced Table 2 and an attenuation threshold of 40 dB.

A synthetic ionogram also has been produced using the program. The resulting curves are presented in Figure 5 and include returns for one, two and three hops together with the corresponding attenuations.

Table 2. Typical Output Listing for Computed Channel Parameters (Includes All Returns for Six or Less Hops)

SUMMARY OF TRANSMISSION PARAMETERS

SIGNAL PARAMETERS

CARRIER FREQ. = 5.000 MHZ. BANDWIDTH = 100.00 MHZ.

TRANSMITTER/RECEIVER PARAMETERS

LOCATION OF TRANSMITTER: LONGITUDE = 150.00 DEGREES (+ FOR WEST, - FOR EAST)  
LATITUDE = 30.00 DEGREES (+ FOR NORTH, - FOR SOUTH)  
DISTANCE BETWEEN TRANSMITTER AND RECEIVER = 500.00 KM.  
DIRECTION FROM TRANSMITTER TO RECEIVER = 0.00 DEGREES (MEASURED FROM TRUE NORTH)  
TRANSMITTER ANTENNA PATTERN = (3/2)\*(SIN(THETA))^2  
RECEIVER ANTENNA PATTERN = (3/2)\*(SIN(THETA))^2  
SEA STATE = 1

IONOSPHERE PARAMETERS

SUNSPOT NUMBER = 100.00  
SOLAR ZENITH ANGLE = 85.00 DEGREES  
DAYTIME ELECTRON DENSITY PROFILE  
E REGION: HEIGHT OF MAX. ELECTRON DENSITY = 110.00 KM.  
PENETRATION FREQUENCY, ORDINARY WAVE = 2.000 MHZ.  
F REGION: PENETRATION FREQUENCY, EXTRAORDINARY WAVE = 2.630 MHZ.  
HEIGHT OF MAX. ELECTRON DENSITY = 250.00 KM.  
PENETRATION FREQUENCY, ORDINARY WAVE = 50.00 KM.  
PENETRATION FREQUENCY, EXTRAORDINARY WAVE = 8.000 MHZ.  
NONDEVIATIVE ABSORPTION CONSTANTS  
MULTIPLICATIVE CONSTANT = 215.00, SUNSPOT NUMBER MULTIPLIER = 0.003500, SOLAR ZENITH ANGLE EXPONENT = 0.750  
DUPLEX REFERENCE VALUES  
E REGION: SHIFT = 0.0100 HZ, SHIFT EXP. = 1.000, SPREAD = 0.0200 HZ, SPREAD EXP. = 1.000, REF. FREQ. = 9.300 MHZ.  
F REGION: SHIFT = 0.0100 HZ, SHIFT EXP. = 1.000, SPREAD = 0.1500 HZ, SPREAD EXP. = 1.000, REF. FREQ. = 9.300 MHZ.

COMPUTED CHANNEL PARAMETERS

GROUNDWAVE: DELAY = 1.847E-03 SEC. ATTENUATION = 1.200E+02 DB.

IONOSPHERE RETURNS

MODE	SOLUTION	RAY ANGLE (DEGREES)	PATH LENGTH (KM)	CARRIER DELAY (SEC)	CARRIER PHASE (CYCLES)	SIGNAL DELAY (SEC)	AMPLITUDE (SEL/MHZ)	PHASE DISTURBANCE (SEC/MHZ**2)	ATTENUATION (DB)	DUPLEX SHIFT (MHZ)	DOPPLER SPREAD (MHZ)
1F0 LOW	0.0	0.00	0.00	0.0	0.0	0.0	0.0	0.0	0.0	0.0	0.0
1F0 HIGH	0.0	0.00	0.00	0.0	0.0	0.0	0.0	0.0	0.0	0.0	0.0
1F1 LOW	1.0	46.91	644.68	2.282E-03	4.094E-01	2.096E-03	5.760E-05	1.346E-05	1.265E+02	5.376E-03	8.065E-02
1F1 HIGH	0.0	0.00	0.00	0.0	0.0	0.0	0.0	0.0	0.0	0.0	0.0
1F2 LOW	1.0	67.53	541.07	1.809E-03	7.755E-01	1.693E-03	1.098E-04	9.042E-05	1.619E+02	5.376E-03	1.075E-02
1F2 HIGH	1.0	58.15	547.19	1.957E-03	4.458E-01	1.161E-03	7.306E-05	1.559E-04	1.465E+02	5.376E-03	1.075E-02
1F3 LOW	1.0	48.11	718.30	2.304E-03	6.671E-01	1.824E-03	1.434E-04	2.562E-05	1.401E+02	5.376E-03	8.065E-02
1F3 HIGH	0.0	0.00	0.00	0.0	0.0	0.0	0.0	0.0	0.0	0.0	0.0
2F0 LOW	0.0	0.00	0.00	0.0	0.0	0.0	0.0	0.0	0.0	0.0	0.0
2F0 HIGH	0.0	0.00	0.00	0.0	0.0	0.0	0.0	0.0	0.0	0.0	0.0
2F1 LOW	1.0	28.55	1046.08	3.847E-03	6.609E-01	3.583E-03	1.991E-04	4.136E-05	1.471E+02	1.075E-02	1.140E-01
2F1 HIGH	0.0	0.00	0.00	0.0	0.0	0.0	0.0	0.0	0.0	0.0	0.0



Table 2. Typical Output Listing for Computed Channel Parameters (Includes All Returns for Six or Less Hops). (Contd.)

[illegible]

Table 3. Index Convention for Ionosphere Returns

Index	Number of Hops	Region	Ordinary or Extraordinary	Low Ray or High Ray
1	1	E	O	LOW
2	1	E	O	HIGH
3	1	F	O	LOW
4	1	F	O	HIGH
5	1	E	X	LOW
6	1	E	X	HIGH
7	1	F	X	LOW
8	1	F	X	HIGH
9	2	E	O	LOW
10	2	E	O	HIGH
11	2	F	O	LOW
.	.	.	.	.
.	.	.	.	.
.	.	.	.	.
44	6	F	O	HIGH
45	6	E	X	LOW
46	6	E	X	HIGH
47	6	F	X	LOW
48	6	F	X	HIGH

Table 4. Glossary of Terms Used  
for Computed Channel Parameters

Mode	Identifies particular ionosphere return (e.g., 2FO LOW is the two-hop, F region, ordinary wave, low ray return)
Solution Indicator	This equals 1 if there is a return for the particular mode and equals 0 if there is no return
Ray Angle	$\theta_j$
Total Path Length	$D_j$
Carrier Delay	$\tau(f_c)$
Carrier Phase	The fractional part of $D_j^{(0)}$
Signal Delay	$D_j^{(1)}$
Amplitude Distortion	$D_j^{(2)}$
Phase Distortion	$D_j^{(3)}$
Attenuation	$L_j$
Doppler Shift	$v_j$
Doppler Spread	$2\sigma_j$

Table 5. Typical Output Listing For Computed Channel Parameters  
(Includes Only Those Returns Having Attenuations Within 40dB Of The Smallest Nonzero Attenuation)

SUMMARY OF TRANSMISSION PARAMETERS

SIGNAL PARAMETERS

CARRIER FREQ. = 5.000 MHZ. BANDWIDTH = 100.00 MHZ.

TRANSMITTER/RECEIVER PARAMETERS

LOCATION OF TRANSMITTER: LONGITUDE = 150.00 DEGREES (+ FOR WEST, - FOR EAST)  
LATITUDE = 30.00 DEGREES (+ FOR NORTH, - FOR SOUTH)  
DISTANCE BETWEEN TRANSMITTER AND RECEIVER = 500.00 KM.  
DIRECTION FROM TRANSMITTER TO RECEIVER = 0.00 DEGREES (MEASURED FROM TRUE NORTH)  
TRANSMITTER ANTENNA PATTERN = (3/2)\*(SIN(THETA))\*\*2  
RECEIVER ANTENNA PATTERN = (3/2)\*(SIN(THETA))\*\*2  
SEA STATE = 1

IONOSPHERE PARAMETERS

SUNSPOT NUMBER = 100.00  
SOLAR ZENITH ANGLE = 45.00 DEGREES  
DAYTIME ELECTRON DENSITY PROFILE  
E REGION: HEIGHT OF MAX. ELECTRON DENSITY = 110.00 KM.  
SMITHKNESS OF PARABOLA = 20.00 KM.  
PENETRATION FREQUENCY, ORDINARY WAVE = 2.000 MHZ.  
F REGION: HEIGHT OF MAX. ELECTRON DENSITY = 250.00 KM.  
SMITHKNESS OF PARABOLA = 50.00 KM.  
PENETRATION FREQUENCY, ORDINARY WAVE = 8.000 MHZ.  
PENETRATION FREQUENCY, EXTRAORDINARY WAVE = 8.537 MHZ.

NONDEVIATIVE ABSORPTION CONSTANTS  
MULTIPLICATIVE CONSTANT = 215.00, SUNSPOT NUMBER MULTIPLIER = 0.003500, SOLAR ZENITH ANGLE EXPONENT = 0.750

DOPPLER REFERENCE VALUES  
E REGION: SHIFT = 0.0100 HZ, SHIFT EXP. = 1.0003, SPREAD = 0.0200 HZ, SPREAD EXP. = 1.0003, RLF, FREQ. = 9.300 MHZ.  
F REGION: SHIFT = 0.0100 HZ, SHIFT EXP. = 1.0003, SPREAD = 0.1200 HZ, SPREAD EXP. = 1.0003, NEF, FREQ. = 9.300 MHZ.

COMPUTED CHANNEL PARAMETERS

GROUNDWAVE DELAY = 1.647E-01 SEC. ATTENUATION = 1.200E+02 DB.

IONOSPHERE RETURNS

MODE	SOLUTION	HAY ANGLE	PATH	CARRIER	CARRIER	SIGNAL	AMPLITUDE	PHASE	ATTENUATION	DUPPLER	DOPPLER
INDICATOR	(0-MO SOLN)	(DEGREES)	LENGTH	DELAY	PHASE	DELAY	(SEC/MHZ)	(DEG/MHZ)**2	(DB)	SHIFT	SPREAD
			(KM)	(SEC)	(CYCLES)	(SEC)	(SEC/MHZ)			(HZ)	(HZ)
1FD LOW	NA	46.91	684.68	2.282E-03	4.094E-01	2.096E-03	5.760E-05	1.346E-05	1.265E+02	5.376E-03	8.065E-02
1FX LOW	NA	67.53	541.07	1.804E-03	7.755E-01	1.933E-03	1.048E-04	9.042E-05	1.619E+02	5.376E-03	1.075E-02
1EX HIGH	NA	58.18	587.19	1.957E-03	4.458E-01	1.616E-03	7.306E-05	-1.595E-04	1.405E+02	5.376E-03	1.075E-02
1FX LOW	NA	44.11	718.30	2.394E-03	6.671E-01	1.824E-03	1.444E-04	2.562E-05	1.401E+02	5.376E-03	8.065E-02
2FD LOW	NA	28.45	1046.08	3.447E-03	6.699E-01	3.583E-03	1.991E-04	4.136E-05	1.471E+02	1.075E-02	1.140E-01

ALL IONOSPHERIC RETURNS WHOSE ATTENUATION IS GREATER THAN 40.00 DB ABOVE THE MINIMUM ATTENUATION ARE IGNORED



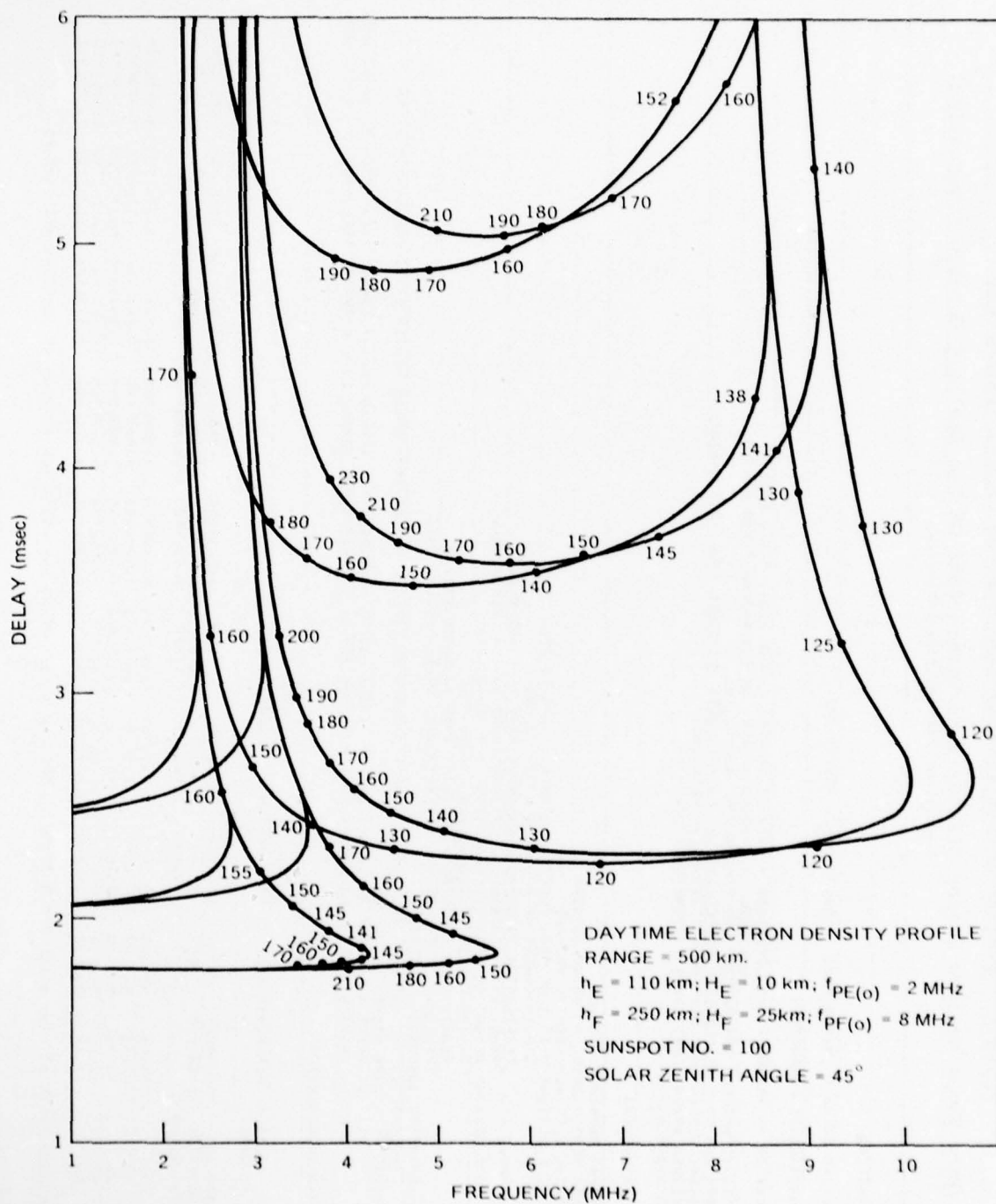


Figure 5. Computed Ionosphere Returns for One, Two and Three Hops  
 (Numbers on Curves are Attenuation in dB)

#### IV. SIGNAL ANALYSIS

This section is concerned with the signal analysis part of the simulator and the approximations used in its implementation. We will assume that the transmitted signal,  $s(t)$ , is bandlimited with (two sided) bandwidth  $BW$ . The received signal,  $r(t)$ , is not strictly bandlimited because it is multiplied by the random gains, which are not bandlimited. However, since the doppler spreads are small compared with the signal bandwidth, the received signal can also be assumed to be bandlimited but with a slightly larger bandwidth than the transmitted signal. The error introduced by this assumption is negligible as long as the assumed bandwidth of the received signal is large compared with the sum of the transmitted signal bandwidth and the largest doppler spread present. In the following we will assume that all signals have a bandwidth equal to twice that of the transmitted signal. This is sufficient to reduce aliasing errors to a negligible value. Denoting the sampling interval associated with this larger bandwidth by  $T_0$  we have

$$T_0 = \frac{1}{2 \cdot BW} \quad (50)$$

As a consequence of the cardinal series representation for band-limited functions, we require a knowledge of the signals involved only at the sample times  $nT_0$ ,  $n = 0, \pm 1, \dots$ . This greatly simplifies the computational and storage requirements. From (21) the received, sampled signal appears as

$$r(nT_0) = A_g s(nT_0 - N_0 T_0) + \sum_{j=1}^N \exp[-2\pi i D_j^{(0)}] \cdot G_j(nT_0) \hat{s}_j(nT_0 - N_j T_0) \quad n=0,1,\dots \quad (51)$$

where the various delays have been replaced by the nearest integer multiple of  $T_0$ . That is,  $N_g$  is defined as the integer satisfying

$$D_g - \frac{1}{2} T_o \leq N_g T_o < D_g + \frac{1}{2} T_o \quad (52)$$

and the  $N_j$ 's are defined as the integers satisfying

$$D_j^{(1)} - \frac{1}{2} T_o \leq N_j T_o < D_j^{(1)} + \frac{1}{2} T_o, \quad j=1, \dots, N. \quad (53)$$

It remains to determine the sampled, distorted signals  $\hat{s}_j(nT_o)$  and the sampled random path gains  $G_j(nT_o)$ .

A. Delay Distortion

The transmitted signal has the representation

$$s(t) = \sum_{n=-\infty}^{\infty} s(nT_o) \frac{\sin 2\pi BW(t-nT_o)}{2\pi BW(t-nT_o)} \quad (54)$$

and the impulse response  $h_j(t)$ , which we also assume to be band-limited, has the representation

$$h_j(t) = \sum_{n=-\infty}^{\infty} h_j(nT_o) \frac{\sin 2\pi BW(t-nT_o)}{2\pi BW(t-nT_o)}, \quad j=1, \dots, N. \quad (55)$$

We obtain the distorted waveform,  $\hat{s}_j(t)$ , by convolving  $s(t)$  and  $h_j(t)$ . But  $\hat{s}_j(t)$  also has an expansion of the above type and

$$\hat{s}_j(t) = \sum_{n=-\infty}^{\infty} \hat{s}_j(nT_o) \frac{\sin 2\pi BW(t-nT_o)}{2\pi BW(t-nT_o)}, \quad j=1, \dots, N. \quad (56)$$

We are interested here in the sample values  $\hat{s}_j(nT_o)$  and these are given by the convolution

$$\hat{s}_j(nT_o) = \sum_{m=-\infty}^{\infty} s(nT_o - mT_o) \hat{h}_j(mT_o), \quad j=1, \dots, N. \quad (57)$$

where

$$\hat{h}_j(mT_0) = T_0 h_j(mT_0) = T_0 \int_{-BW}^{BW} H_j(f) \exp[2\pi i f m T_0] df. \quad (58)$$

$j=1, \dots, N$

The transfer function  $H_j(f)$  is given by (11), and it will be approximated with the first two terms of the series appearing in the exponent, that is

$$H_j(f) \approx \exp[-2\pi i f^2 D_j^{(2)} - 2\pi i f^3 D_j^{(3)}], \quad j=1, \dots, N. \quad (59)$$

After the change of variable  $\eta = f/BW$ , we obtain from (58)

$$\hat{h}_j(mT_0) \approx \frac{1}{2} \int_{-1}^1 \exp[-i\Delta_j^{(2)} \eta^2 - i\Delta_j^{(3)} \eta^3] \cdot \exp[i m \pi \eta] d\eta \quad (60)$$

$j=1, \dots, N$

with

$$\Delta_j^{(2)} = 2\pi (BW)^2 D_j^{(2)} \quad (61)$$

$$\Delta_j^{(3)} = 2\pi (BW)^3 D_j^{(3)}. \quad (62)$$

Closed form expressions for (60) are not known and further approximations are required for the numerical determination of  $\hat{h}_j(mT_0)$ . Let  $I(x)$  represent the general integral defining the impulse responses, that is

$$I(x) = \frac{1}{2} \int_{-1}^1 \exp[-i\Delta^{(2)} \eta^2 - i\Delta^{(3)} \eta^3] \cdot \exp[ix\eta] d\eta. \quad (63)$$

Expanding  $\exp[-i\Delta^{(3)} \eta^3]$  in a power series we have the representation



$$I(x) = \sum_{p=0}^{\infty} \frac{(-i\Delta^{(3)})^p}{p!} I_p(x) \quad (64)$$

where we have defined

$$I_p(x) = \frac{1}{2} \int_{-1}^1 \eta^{3p} \exp[-i\Delta^{(2)} \eta^2] \cdot \exp[ix\eta] d\eta \quad (65)$$

The integral  $I_0(x)$  is readily expressed in terms of Fresnel integrals [24]. For the higher order integrals the following recurrence relation has been derived

$$I_p(x) = \frac{i}{4\Delta^{(2)}} \exp[-i\Delta^{(2)}] \left\{ \exp[ix] + (-1)^p \exp[-ix] \right\} \\ + \frac{x}{2\Delta^{(2)}} I_{p-1}(x) - i \frac{(p-1)}{2\Delta^{(2)}} I_{p-2}(x), \quad p \geq 1. \quad (66)$$

where we have adopted the convention that  $I_{-1}(x) = 0$ .

The impulse responses for the ionosphere returns can now be evaluated with relative ease. Starting with  $I_0(x)$  and using (66) we determine as many of the terms  $I_p(x)$  as are needed to adequately approximate the infinite sum (64). The integral  $I_0(x)$  is evaluated using the rational approximation presented in [25]. Care must be exercised in implementing this procedure, however. The error incurred by using the rational approximation for  $I_0(x)$  is approximately  $1.0 \times 10^{-9}$ . For large arguments ( $x > 5$ ) nearly equal functions are subtracted in (66) and this reduces the number of significant figures in the resulting expression. For the higher order terms this reduction in the number of significant figures is important and the computed values may become inaccurate. It is evident from (64) that this effect will be more noticeable when  $\Delta^{(3)}$  is large. Experience has shown that values of  $x$  as large as 20-25 can be tolerated in most applications before the errors become excessive.

## B. Random Gains

The random gains,  $G_j(t)$ , in the ionosphere returns are complex valued, zero mean, Gaussian processes whose correlation function and power spectral density are given by (cf. Eqns. 19 and 20)

$$C_{G_j}(\tau) = A_j^2 \exp[-2\pi^2 \sigma_j^2 \tau^2 + 2\pi i v_j \tau] , j=1, \dots, N \quad (67)$$

and

$$P_{G_j}(f) = \frac{A_j^2}{\sqrt{2\pi}\sigma_j} \exp\left[-\frac{(f-v_j)^2}{2\sigma_j^2}\right] , j=1, \dots, N. \quad (68)$$

We wish to generate a random sequence with the above correlation function and we wish to do this directly in the time domain and not rely on Fourier transform techniques. Because the doppler spreads,  $\sigma_j$ , are small relative to the signal bandwidths, the time domain approach requires a large memory. To avoid these large memory requirements we will replace the original process with an approximation that can be generated more easily.

The approximate random gain will be denoted by  $\tilde{G}_j(t)$  and it will be chosen to have the power spectral density

$$P_{\tilde{G}_j}^{\sim}(f) = \frac{8A_j^2}{3\pi\rho\sigma_j} \frac{1}{\left[1 + \left(\frac{f-v_j}{\rho\sigma_j}\right)^2\right]^3} , j=1, \dots, N \quad (69)$$

and corresponding correlation function

$$C_{\tilde{G}_j}^{\sim}(\tau) = A_j^2 \left[1 + 2\pi\rho\sigma_j|\tau| + \frac{1}{3}(2\pi\rho\sigma_j|\tau|)^2\right] \cdot \exp\left[-2\pi\rho\sigma_j|\tau| + 2\pi i v_j \tau\right] , j=1, \dots, N. \quad (70)$$

The parameter  $\rho$  is chosen so that (70) agrees with (67) over a reasonable range of arguments. The value  $\rho = 2.1$  has been determined to be a good choice and this is the value that will be used

throughout the following. Normalized plots of  $C_{G_j}(\tau)$  and  $C_{G_j}^v(\tau)$  are compared in Figure 6.

It is obvious from (69) that the approximate process  $\hat{G}_j(t)$  is not bandlimited. However, the error introduced by assuming that the process has bandwidth BW will be negligible since  $(\sigma_j/BW) \ll 1$ . Accordingly we will treat  $\hat{G}_j(t)$  as if it is bandlimited, in which case we need only evaluate it at the sample times  $nT_o$ . Thus, the original problem has been reduced to the generation of a complex valued, zero mean, Gaussian sequence with correlation function

$$C_{G_j}^v(nT_o) = A_j^2 \left[ 1 + 2\pi\rho\sigma_j T_o |n| + \frac{1}{3} (2\pi\rho\sigma_j T_o |n|)^2 \right] \cdot \exp \left[ -2\pi\rho\sigma_j T_o |n| + 2\pi i v_j T_o n \right] \quad (71)$$

$n=0, \pm 1, \dots$   
 $j=1, \dots, N$

The technique used for the computer generation of the approximate process is discussed in Appendix C. A plot of the normalized, empirical correlation function of the computer-generated process is also displayed in Figure 6. Agreement between the computer-generated correlation function and the approximate correlation function (71) is excellent for the range of arguments considered.

### C. Computer Program

A listing of the Fortran program used to implement the signal analysis part of the simulator is presented in Appendix D. Channel parameter information is read into the program via data cards that have been produced by the first part of the simulator. The sampled input values are read from a tape, the program calculates the sampled output values according to Eqn. (51) and writes the output on another tape. As an alternate, printed output also can be obtained, but, because the quantity of output data is large, the usefulness of this mode of presentation is severely limited.

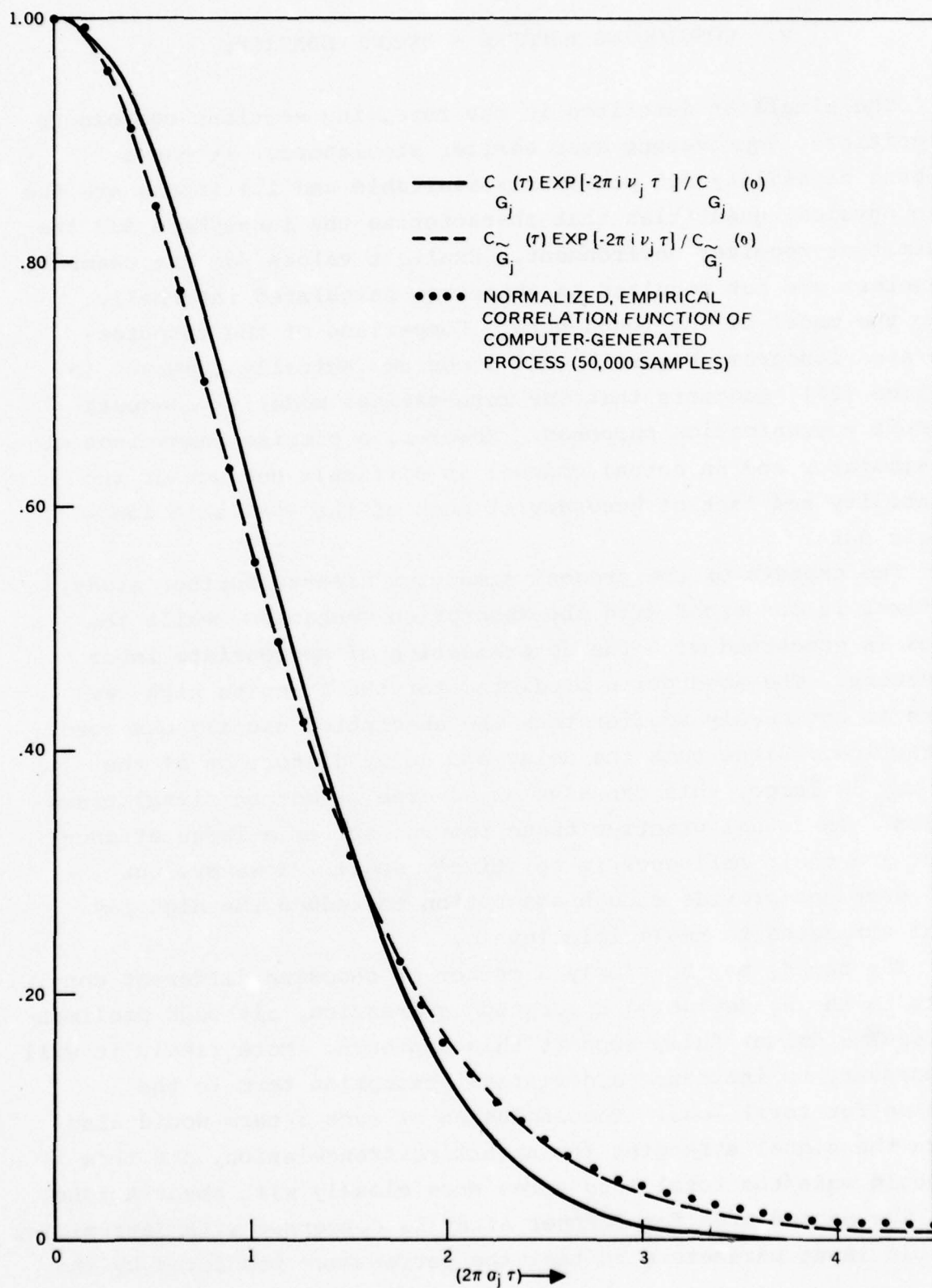


Figure 6. Normalized Correlation Function for the Random Gains



## V. CONCLUDING REMARKS - RECOMMENDATIONS

The simulator described in the foregoing sections represents a significant improvement over earlier simulators. It has a wideband capability not previously available and its inputs are the basic physical quantities that characterize the ionosphere and the transmitter-receiver environment. Explicit values for the channel parameters are not required as these are calculated internally using the model of the ionosphere. Comparison of the computer-generated ionogram, Figure 5, and ionograms actually observed in practice [27], suggests that our mathematical model is adequate for most communication purposes. However, a precise comparison of the simulator and an actual channel is difficult because of the variability and lack of accuracy of much of the available ionospheric data.

Two aspects of the present simulator deserve further study. The first is concerned with the absorption mechanism, while the second is concerned with the determination of appropriate input parameters. The absorption predicted for the F region high ray return is noticeably smaller than the absorption usually observed in practice. Since both the delay and delay distortion of the high ray is large, this can have an adverse affect on signal transmission. In actual practice these returns suffer a large attenuation, and their influence is relatively small. However, our model does not provide enough absorption to reduce the high ray signal strengths to negligible levels.

The remedy may be simply a matter of choosing different constants in the nondeviative absorption expression, although preliminary results do not fully support this approach. More likely it will be necessary to introduce a deviative absorption term in the equation for total loss. The inclusion of such a term would also reduce the signal strengths for nighttime transmission, and this too would make the total loss agree more closely with observations.

The second area for further study is concerned with determining suitable input parameters so that the performance predicted by the

mathematical model agrees as well as possible with the actual observed performance. This involves matching actual and computer-generated observables such as doppler shift, doppler spread, attenuation and delay vs. frequency plots (ionograms) to determine the input parameters. Besides the obvious advantage of providing further justification of the assumptions used in the model, this parameter determination would provide the user with a set of inputs that correspond to a variety of actual environments.

The primary difficulty encountered in the determination of the input parameters is that an explicit functional relationship does not exist between the input parameters and the computed channel parameters; the channel parameters are determined by numerically solving a transcendental equation. As a consequence, techniques must be developed that are tailored to the ionosphere model. One approach is to select the most significant observable features and to determine the relationship between these features and the input parameters. For example, the nearly horizontal portions of an observed ionogram would be affected most by the heights of the regions and to a lesser degree by the thickness of the regions and their peak electron densities. On the other hand, the maximum operating frequency is likely to be more affected by the peak electron densities than the heights or thicknesses of the regions. A detailed study of these and other pertinent relationships would provide the user with the ability to determine input parameters corresponding to a variety of observed operating conditions. These same conditions could then be reproduced by the channel simulator as required for system studies.

## VI REFERENCES

- [1] C.C. Watterson, J.R. Juroshek and W.D. Benesema, "Experimental Confirmation of an HF Channel Model," IEEE Transactions on Communication Technology, Vol. COM-18, pp. 792-803, 1970.
- [2] W.F. Walker, "Baseband Multipath Fading Simulator," Radio Science, Vol. 1, pp. 763-767, 1966.
- [3] R. Cole, W.M. Jewett and J.W. Linnehan, Jr., "A Programmable Real-Time HF Channel Simulator," Proceedings of the Sixth Annual Conference on Modeling and Simulation, pp. 259-266, 1975.
- [4] K.K. Clarke, "Random Channel Simulation and Instrumentation," IEEE Communications Convention Record, pp. 623-629, 1965.
- [5] D.B. Sailors and J.R. Hill, "Simulation and Measurement of High Frequency Ionospheric Channels," NOSC Technical Report 111, April 1977.
- [6] K.G. Gray and S.A. Bowhill, "The Impulse Response of a Cold Stratified Plasma in the Presence of Collisions and a Vertical Magnetic Field by a Multiple-Scattering Technique," Radio Science, Vol. 9, pp. 559-566, 1974.
- [7] K.G. Gray and S.A. Bowhill, "Transient Response of Stratified Media: Multiple-Scattering Integral and Differential Equations for an Impulsive Incident Plane Wave," Radio Science, Vol. 9, pp. 57-62, 1974.
- [8] K.G. Gray and S.A. Bowhill, "Transient Response of Stratified Media: Response to an Arbitrary Incident Plane Wave," Radio Science, Vol. 9, pp. 63-69, 1974.
- [9] K.G. Gray, "An Integral Equation for the Transient Response of a Stratified Magnetoplasma," IEEE Transactions on Antennas and Propagation, Vol. 24, pp. 539-541, 1976.
- [10] D.A. Hill and J.R. Wait, "Theory of the Electromagnetic Transient Response of the Ionosphere for Plane Wave Excitation," Pure and Applied Geophysics, Vol. 90, pp. 169-186, 1971.
- [11] S.O. Rice, "Mathematical Analysis of Random Noise," Bell System Technical Journal, Vol. 23, pp. 282-332 and Vol. 24, pp. 46-156, 1944 and 1945.
- [12] H.N. Shaver, B.C. Tupper and J.B. Lomax, "Evaluation of a Gaussian HF Channel Model," IEEE Transactions on Communication Technology, Vol. COM-15, pp. 79-88, 1967.



- [13] J.T. Boys, "Statistical Variations in the Apparent Specular Component of Ionospherically Reflected Radio Waves," Radio Science, Vol. 3, pp. 984-990, 1968.
- [14] M. Balser and W.B. Smith, "Some Statistical Properties of Pulsed Oblique HF Ionospheric Transmissions," Journal of Research of the National Bureau of Standards, Vol. 66D, pp. 721-730, 1962.
- [15] D.E. Barrick, "Theory of Ground-Wave Propagation Across a Rough Sea at Dekameter Wavelengths," Battelle Memorial Institute Report, Contract DAAH01-70-C-0312, 1970.
- [16] K. Davies, Ionospheric Radio Propagation, National Bureau of Standards Monograph 80, U.S. Government Printing Office, Washington, D.C., 1965.
- [17] I.S. Gradshteyn and I.M. Ryzhik, Table of Integrals, Series and Products, Academic Press, New York, 1965.
- [18] R. A. Shepherd and J.B. Lomax, "Frequency Spread in Ionospheric Radio Propagation," IEEE Transactions on Communication Technology, Vol. COM-15, pp. 268-275, 1967.
- [19] P.A. Fialer, "Irregularities in the Quiet Ionosphere and their Effect on Propagation," Technical Report No. 156, Radio Science Laboratory, Stanford Electronics Laboratories, Stanford University, 1970.
- [20] W. Pfister, "The Wave-Like Nature of Inhomogeneities in the E-Region," Journal of Atmospheric and Terrestrial Physics, Vol. 33, pp. 999-1025, 1971.
- [21] F. David, A.G. Franco, H. Sherman and L.B. Shucavage, "Correlation Measurements on HF Transmission Link," IEEE Transactions on Communication Technology, Vol. COM-17, pp. 245-394, 1967.
- [22] K. Davies, "The Measurement of Ionospheric Drifts by Means of a Doppler Shift Technique," Journal of Geophysical Research, Vol. 67, pp. 4909-4913, 1962.
- [23] K. Davies and D.M. Baker, "On Frequency Variations of Ionospherically Propagated HF Radio Signals," Radio Science, Vol. 1, pp. 545-556, 1966.
- [24] M. Abramowitz and I.A. Stegun, Handbook of Mathematical Functions, National Bureau of Standards, Applied Mathematics Series No. 55, U.S. Government Printing Office, Washington, 1964.



- [25] J. Boersma, "Computation of Fresnel Integrals," Math. Comp., Vol. 14, p. 380, 1960.
- [26] E. Parzen, Stochastic Processes, Holden Day, San Francisco, 1962.
- [27] J.E. Hipp and T.C. Green, "Measured Sea Path Sky Wave/Ground Wave Signal Power Ratios over the 2-10 mHz Range," Southwest Research Institute Task Report XXXIII, Contract N00039-72-C-1275, Naval Electronic Systems Command, 1976.

APPENDIX A  
DELAY AND DELAY DERIVATIVES

# APPENDIX A DELAY AND DELAY DERIVATIVES

In this appendix we present the equations for the delay and the first three delay derivatives. Recalling the definition of  $A(x)$  we have

$$A(x) = 2G \left( \frac{1-x^2}{x} \right)^{\frac{1}{2}} \quad (\text{A.1})$$

where  $x = \cos \theta$ . We must solve the equation

$$R = A(x) \quad (\text{A.2})$$

with  $R$  equal to the distance between transmitter and receiver. The solution then yields the delay via the equation

$$\tau = \frac{R}{c(1-x^2)^{\frac{1}{2}}} \quad (\text{A.3})$$

with  $c$  the velocity of light. The delay derivatives are given by

$$\frac{d\tau}{df} = \frac{x\tau}{(1-x^2)} \frac{dx}{df} \quad (\text{A.4})$$

$$\frac{d^2\tau}{df^2} = \frac{1+2x^2}{x^2\tau} \left( \frac{d\tau}{dx} \right)^2 + \frac{x\tau}{(1-x^2)} \frac{d^2x}{df^2} \quad (\text{A.5})$$

and

$$\begin{aligned} \frac{d^3\tau}{df^3} = & - \frac{3(1+x^2+2x^4)}{x^4\tau^2} \left( \frac{d\tau}{df} \right)^2 + \frac{3(1+2x^2)}{x^2\tau} \left( \frac{d\tau}{df} \right) \left( \frac{d^2\tau}{df^2} \right) \\ & + \frac{x\tau}{(1-x^2)} \frac{d^3x}{df^3} . \end{aligned} \quad (\text{A.6})$$

Thus to determine the delay and delay derivatives we must solve (A.2) for  $x$  and then evaluate the first three derivatives of  $x$  with respect to  $f$  for use in (A.4) - (A.6). In the following these functions are listed for the two electron density profiles. The group height  $G(x)$  is obtained by evaluating the integral (24).

#### 1. Nighttime

For the nighttime electron density the integral for the group height is evaluated and used in (A.1) to yield

$$A(x) = \begin{cases} 2\left(\frac{1-x^2}{x^2}\right)^{\frac{1}{2}} \left\{ h_E - 2H_E + H_E \hat{f}_E x \ln \left( \frac{1+\hat{f}_E x}{1-\hat{f}_E x} \right) \right\}, & \hat{f}_E x \leq 1 \\ 2\left(\frac{1-x^2}{x^2}\right)^{\frac{1}{2}} \left\{ h_F - 2H_F - 4H_E + 2H_E \hat{f}_E x \ln \left( \frac{\hat{f}_E^{x+1}}{\hat{f}_E^{x-1}} \right) \right. \\ \quad \left. + H_F \hat{f}_F x \ln \left( \frac{1+\hat{f}_F x}{1-\hat{f}_F x} \right) \right\}, & \hat{f}_E x > 1 \end{cases} \quad (A.7)$$

where

$$\hat{f}_E = \frac{f}{f_{pE}} \text{ and } \hat{f}_F = \frac{f}{f_{pF}}.$$

For  $\hat{f}_E x \leq 1$  the derivatives of  $x$  with respect to frequency are:

$$\frac{dx}{df} = \left(\frac{x}{f}\right) \cdot \frac{R \cdot \left(\frac{x^2}{1-x^2}\right)^{\frac{1}{2}} - \left[ 2h_E - \frac{4H_E}{1-\hat{f}_E^2 x^2} \right]}{R \cdot \left(\frac{x^2}{1-x^2}\right)^{\frac{3}{2}} + \left[ 2h_E - \frac{4H_E}{1-\hat{f}_E^2 x^2} \right]}, \quad \hat{f}_E x \leq 1 \quad (A.8)$$



$$\frac{d^2x}{df^2} = \frac{1}{x} \left( \frac{dx}{df} \right)^2 - \frac{1}{f} \left( \frac{dx}{df} \right)$$

$$+ \frac{\left( \frac{x}{f} \right) \cdot \frac{R \cdot \left( \frac{1}{1-x^2} \right)^{\frac{3}{2}} \left( \frac{dx}{df} \right) \left[ 1 - \frac{3xf}{1-x^2} \frac{dx}{df} \right] + \frac{8H_E f \hat{f}_E^2 \left( \frac{x}{f} + \frac{dx}{df} \right)}{(1-\hat{f}_E^2 x^2)^2}}{R \cdot \left( \frac{x^2}{1-x^2} \right)^{\frac{3}{2}} + \left[ 2h_E - \frac{4H_E}{1-\hat{f}_E^2 x^2} \right]}, \quad \hat{f}_E x \leq 1. \quad (A.9)$$

$$\frac{d^3x}{df^3} = -\frac{1}{x^2} \left( \frac{dx}{df} \right)^3 + \frac{2}{x} \left( \frac{dx}{df} \right) \left( \frac{d^2x}{df^2} \right) + \frac{1}{f^2} \left( \frac{dx}{df} \right) - \frac{1}{f} \left( \frac{d^2x}{df^2} \right)$$

$$- \frac{1}{x} \left( \frac{x}{f} - \frac{dx}{df} \right) \left[ \frac{d^2x}{df^2} - \frac{1}{x} \left( \frac{dx}{df} \right)^2 + \frac{1}{f} \frac{dx}{df} \right]$$

$$- \frac{\left[ \frac{d^2x}{df^2} - \frac{1}{x} \left( \frac{dx}{df} \right)^2 + \frac{1}{f} \frac{dx}{df} \right]}{R \cdot \left( \frac{x^2}{1-x^2} \right)^{\frac{3}{2}} + \left[ 2h_E - \frac{4H_E}{1-\hat{f}_E^2 x^2} \right]} \left\{ \frac{3R \cdot x^2 \left( \frac{dx}{df} \right)}{(1-x^2)^{\frac{5}{2}}} - \frac{8H_E x \hat{f}_E^2 \left( \frac{x}{f} + \frac{dx}{df} \right)}{(1-\hat{f}_E^2 x^2)^2} \right\}$$

$$+ \frac{\left( \frac{x}{f} \right)}{R \cdot \left( \frac{x^2}{1-x^2} \right)^{\frac{3}{2}} + \left[ 2h_E - \frac{4H_E}{1-\hat{f}_E^2 x^2} \right]} \left\{ \frac{R}{(1-x^2)^{\frac{5}{2}}} \left[ 1 - \frac{3xf}{1-x^2} \frac{dx}{df} \right] \right.$$

$$\cdot \left[ 3x \left( \frac{dx}{df} \right)^2 + (1-x^2) \frac{d^2x}{df^2} \right]$$

$$- \frac{3Rf \left( \frac{dx}{df} \right)}{(1-x^2)^{\frac{5}{2}}} \left[ \frac{1+x^2}{1-x^2} \left( \frac{dx}{df} \right)^2 + \left( \frac{x}{f} \right) \frac{dx}{df} + x \frac{d^2x}{df^2} \right]$$

$$+ \frac{32H_E x f \hat{f}_E^4 \left( \frac{x}{f} + \frac{dx}{df} \right)^3}{(1-\hat{f}_E^2 x^2)^3}$$

$$+ \frac{8H_E \hat{f}_E^2 \left( \frac{x}{f} + \frac{dx}{df} \right)}{(1-\hat{f}_E^2 x^2)^2} \left[ \frac{x}{f} + 5 \frac{dx}{df} + 2 f \frac{d^2x}{df^2} \right] \left. \right\}, \quad \hat{f}_E x \leq 1. \quad (A.10)$$

For  $\hat{f}_E x > 1$  these derivatives appear as

$$\frac{dx}{df} = \left(\frac{x}{f}\right) \cdot \frac{F \cdot \left(\frac{x^2}{1-x^2}\right)^{\frac{1}{2}} - \left[2h_F + \frac{8H_E}{\hat{f}^2 E x^2 - 1} - \frac{4H_F}{1 - \hat{f}^2 F x^2}\right]}{F \cdot \left(\frac{x^2}{1-x^2}\right)^{\frac{3}{2}} + \left[2h_F + \frac{8H_E}{\hat{f}^2 E x^2 - 1} - \frac{4H_F}{1 - \hat{f}^2 F x^2}\right]}, \quad \hat{f}_E x > 1 \quad (A.11)$$

$$\frac{d^2 x}{df^2} = \frac{1}{x} \left(\frac{dx}{df}\right)^2 - \frac{1}{f} \left(\frac{dx}{df}\right)$$

$$+ \left(\frac{x}{f}\right) \cdot \frac{R \cdot \left(\frac{dx}{df}\right) \left[1 - \frac{3xf}{1-x^2} \frac{dx}{df}\right] + \frac{16H_E f \hat{f}^2 E \left(\frac{x}{f} + \frac{dx}{df}\right)^2}{(\hat{f}^2 E x^2 - 1)^2} + \frac{8H_F f \hat{f}^2 F \left(\frac{x}{f} + \frac{dx}{df}\right)^2}{(1 - \hat{f}^2 F x^2)^2}}{R \cdot \left(\frac{x^2}{1-x^2}\right)^{\frac{3}{2}} + \left[2h_F + \frac{8H_E}{\hat{f}^2 E x^2 - 1} - \frac{4H_F}{1 - \hat{f}^2 F x^2}\right]}, \quad \hat{f}_E x > 1 \quad (A.12)$$

$$\frac{d^3 x}{df^3} = -\frac{1}{x^2} \left(\frac{dx}{df}\right)^3 + \frac{2}{x} \left(\frac{dx}{df}\right) \left(\frac{d^2 x}{df^2}\right) + \frac{1}{f^2} \left(\frac{dx}{df}\right) - \frac{1}{f} \left(\frac{d^2 x}{df^2}\right)$$

$$- \frac{1}{x} \left(\frac{x}{f} - \frac{dx}{df}\right) \left[\frac{d^2 x}{df^2} - \frac{1}{x} \left(\frac{dx}{df}\right)^2 + \frac{1}{f} \frac{dx}{df}\right]$$

$$- \frac{\left[\frac{d^2 x}{df^2} - \frac{1}{x} \left(\frac{dx}{df}\right)^2 + \frac{1}{f} \frac{dx}{df}\right]}{R \cdot \left(\frac{x^2}{1-x^2}\right)^{\frac{3}{2}} + \left[2h_F + \frac{8H_E}{\hat{f}^2 E x^2 - 1} - \frac{4H_F}{1 - \hat{f}^2 F x^2}\right]} \left\{ \frac{3R x^2 \left(\frac{dx}{df}\right)}{(1-x^2)^{\frac{3}{2}}}\right.$$

$$\left. - \frac{16H_E x \hat{f}^2 E \left(\frac{x}{f} + \frac{dx}{df}\right)}{(\hat{f}^2 E x^2 - 1)^2} - \frac{8H_F x \hat{f}^2 F \left(\frac{x}{f} + \frac{dx}{df}\right)}{(1 - \hat{f}^2 F x^2)^2} \right\}$$

$$\begin{aligned}
& + \frac{\frac{x}{f}}{R \cdot \left( \frac{x^2}{1-x^2} \right)^{\frac{3}{2}} + \left[ 2h_F + \frac{8H_E}{\hat{f}_E^2 x^2 - 1} - \frac{4H_F}{1 - \hat{f}_F^2 x^2} \right]} \\
& \cdot \left\{ \frac{R \cdot \left[ 1 - \frac{3xf}{1-x^2} \frac{dx}{df} \right]}{(1-x^2)^{\frac{5}{2}}} \left[ 3x \left( \frac{dx}{df} \right)^2 + (1-x^2) \left( \frac{d^2x}{df^2} \right) \right] \right. \\
& - \frac{3Rf \left( \frac{dx}{df} \right)}{(1-x^2)^{\frac{5}{2}}} \left[ \frac{1+x^2}{1-x^2} \left( \frac{dx}{df} \right)^2 + \left( \frac{x}{f} \right) \frac{dx}{df} + x \frac{d^2x}{df^2} \right] \\
& - \frac{64H_E x f \hat{f}_E^4 \left( \frac{x}{f} + \frac{dx}{df} \right)^3}{(\hat{f}_E^2 x^2 - 1)^3} + \frac{32H_F x f \hat{f}_F^4 \left( \frac{x}{f} + \frac{dx}{df} \right)^3}{(1 - \hat{f}_F^2 x^2)^3} \\
& + \frac{16H_E \hat{f}_E^2 \left( \frac{x}{f} + \frac{dx}{df} \right) \left[ \frac{x}{f} + 5 \frac{dx}{df} + 2f \frac{d^2x}{df^2} \right]}{(\hat{f}_E^2 x^2 - 1)^2} \\
& + \frac{8H_F \hat{f}_F^2 \left( \frac{x}{f} + \frac{dx}{df} \right) \left[ \frac{x}{f} + 5 \frac{dx}{df} + 2f \frac{d^2x}{df^2} \right]}{(1 - \hat{f}_F^2 x^2)^2} , \quad f_E x > 1. \quad (A.13)
\end{aligned}$$

## 2. Daytime

The daytime electron density profile differs from the nighttime profile only for heights greater than  $h_E$ . Thus the daytime equations for  $\hat{f}_E < 1$  are the same as the nighttime equations. In this case

$$A(x) = \begin{cases} 2 \left( \frac{1-x^2}{x^2} \right)^{\frac{1}{2}} \left\{ h_E - 2H_E + H_E \hat{f}_E x \ln \left( \frac{1+\hat{f}_E x}{1-\hat{f}_E x} \right) \right\}, & \hat{f}_E x \leq 1 \\ 2 \left( \frac{1-x^2}{x^2} \right)^{\frac{1}{2}} \left\{ h_E - 2H_E + H_E \hat{f}_E x \ln \left( \frac{\hat{f}_E x + 1}{\hat{f}_E x - 1} \right) \right. \\ \quad + \left[ h_F - h_E - 2H_F (1-r^2)^{\frac{1}{2}} \right] \left( \frac{\hat{f}_E^2 x^2}{\hat{f}_E^2 x^2 - 1} \right)^{\frac{1}{2}} \\ \quad \left. + 2H_F \hat{f}_F x \ln \left[ \frac{(1-r^2)^{\frac{1}{2}} + (\hat{f}_F^2 x^2 - r^2)^{\frac{1}{2}}}{(1-\hat{f}_F^2 x^2)^{\frac{1}{2}}} \right] \right\}, & \hat{f}_E x > 1 \end{cases} \quad (A.14)$$

where

$$r^2 = \frac{f_{pE}^2}{f_{pF}^2}.$$

For  $\hat{f}_E x \leq 1$  the derivatives of  $x$  with respect to frequency are given by (A.8) - (A.10). For  $\hat{f}_E x > 1$  we have

$$\frac{dx}{df} = \left( \frac{x}{\hat{f}} \right) \frac{R \cdot \left( \frac{x^2}{1-x^2} \right)^{\frac{1}{2}} - B(x)}{R \cdot \left( \frac{x^2}{1-x^2} \right)^{\frac{3}{2}} + B(x)}, \quad \hat{f}_E x > 1 \quad (A.15)$$

with  $B(x)$  defined by

$$B(x) = 2h_E + \frac{4H_E}{\hat{f}_E^2 x^2 - 1} + 2 \left( h_F - h_E - 2H_F \sqrt{1-r^2} \right) \cdot \left( \frac{\hat{f}_E^2 x^2}{\hat{f}_E^2 x^2 - 1} \right)^{\frac{3}{2}} \\ - \frac{4H_F \hat{f}_F^3 x^3}{\sqrt{1-r^2} (\hat{f}_F^2 x^2 - r^2)^{\frac{1}{2}} + (\hat{f}_F^2 x^2 - r^2)} - \frac{4H_F \hat{f}_F^3 x^3}{1 - \hat{f}_F^2 x^2} \quad (A.16)$$



$$\frac{d^2 x}{df^2} = \frac{1}{x} \left( \frac{dx}{df} \right)^2 - \frac{1}{f} \frac{dx}{df}$$

$$+ \frac{R \left( \frac{x}{f} \right) \frac{dx}{df} \left[ 1 - \frac{3xf}{1-x^2} \frac{dx}{df} \right] - \left( \frac{x}{f} + \frac{dx}{df} \right) \frac{dB(x)}{df}}{R \cdot \left( \frac{x^2}{1-x^2} \right)^{\frac{3}{2}} + B(x)}, \quad \hat{f}_E x > 1 \quad (A.17)$$

$$\frac{dB(x)}{df} = \left( \frac{x}{f} + \frac{dx}{df} \right) \cdot \left\{ \frac{8H_E \hat{f}_E^2 x}{(\hat{f}_E^2 x^2 - 1)^2} - 6(h_F - h_E - 2H_F \sqrt{1-r^2}) \frac{\hat{f}_E^3 x^2}{(\hat{f}_E^2 x^2 - 1)^{\frac{5}{2}}} \right.$$

$$- \frac{12H_F \hat{f}_F^3 x^2}{\sqrt{1-r^2} (\hat{f}_F^2 x^2 - r^2)^{\frac{1}{2}} + (\hat{f}_F^2 x^2 - r^2)}$$

$$+ \frac{4H_F \hat{f}_F^5 x^4 \left[ 2 + \sqrt{1-r^2} (\hat{f}_F^2 x^2 - r^2)^{-\frac{1}{2}} \right]}{\left[ \sqrt{1-r^2} (\hat{f}_F^2 x^2 - r^2)^{\frac{1}{2}} + (\hat{f}_F^2 x^2 - r^2) \right]^2}$$

$$- \frac{4H_F \hat{f}_F^3 x^2 (3 - \hat{f}_F^2 x^2)}{(1 - \hat{f}_F^2 x^2)^2} \left. \right\} \quad (A.18)$$

$$\frac{d^3 x}{df^3} = -\frac{1}{x^2} \left( \frac{dx}{df} \right)^3 + \frac{2}{x} \left( \frac{dx}{df} \right) \left( \frac{d^2 x}{df^2} \right) + \frac{1}{f^2} \frac{dx}{df} - \frac{1}{f} \frac{d^2 x}{df^2}$$

$$+ \frac{1}{R \cdot \left( \frac{x^2}{1-x^2} \right)^{3/2} + B(x)} \left\{ -\frac{3R x \left( \frac{dx}{df} \right)}{(1-x^2)^{5/2}} \left[ \frac{1+4x^2}{1-x^2} \left( \frac{dx}{df} \right)^2 + \left( \frac{x}{f} \right) \left( \frac{dx}{df} \right) + 3x \frac{d^2 x}{df^2} \right] \right.$$

$$+ \frac{R}{f \cdot (1-x^2)^{3/2}} \left[ \frac{1+2x^2}{1-x^2} \left( \frac{dx}{df} \right)^2 - \left( \frac{x}{f} \right) \frac{dx}{df} + x \frac{d^2 x}{df^2} \right]$$

$$- \frac{1}{f} \frac{dB(x)}{df} \left[ 2 \frac{dx}{df} - \frac{x}{f} + 2f \frac{d^2 x}{df^2} - \frac{f}{x} \left( \frac{dx}{df} \right)^2 \right]$$

$$- \left( \frac{x}{f} + \frac{dx}{df} \right) \frac{d^2 B(x)}{df^2} \left\{ , \hat{f}_E x > 1 \right. \quad (A.19)$$

$$\frac{d^2 B(x)}{df^2} = \frac{1}{f} \frac{\frac{dB(x)}{df}}{\left( \frac{x}{f} + \frac{dx}{df} \right)} \left[ \frac{dx}{df} - \frac{x}{f} + f \frac{d^2 x}{df^2} \right]$$

$$+ \left( \frac{x}{f} + \frac{dx}{df} \right) \left\{ -\frac{8H_E \hat{f}_E^2}{(\hat{f}_E^2 x^2 - 1)^3} \left[ \hat{f}_E^2 x^2 \left( 2 \frac{x}{f} + 3 \frac{dx}{df} \right) + 2 \left( \frac{x}{f} + \frac{dx}{df} \right) \right] \right.$$

$$+ \frac{6\hat{f}_E^3 x (h_F - h_E - 2H_F \sqrt{1-r^2})}{(\hat{f}_E^2 x^2 - 1)^{3/2}} \left[ \hat{f}_E^2 x^2 \left( 2 \frac{x}{f} + 3 \frac{dx}{df} \right) + \left( 3 \frac{x}{f} + 2 \frac{dx}{df} \right) \right]$$

$$\begin{aligned}
& + \frac{12H_F \hat{f}_F^3 x \left[ -\left(3 \frac{x}{\hat{f}} + 2 \frac{dx}{d\hat{f}}\right) + \hat{f}_F^2 x^2 \left(\frac{x}{\hat{f}} + \frac{dx}{d\hat{f}}\right) \right] \left[ 2 + \sqrt{1-r^2} (\hat{f}_F^2 x^2 - r^2)^{-\frac{1}{2}} \right]}{\sqrt{1-r^2} (\hat{f}_F^2 x^2 - r^2)^{\frac{1}{2}} + (\hat{f}_F^2 x^2 - r^2)} \\
& + \frac{4H_F \hat{f}_F^5 x^3 \left( 5 \frac{x}{\hat{f}} + 4 \frac{dx}{d\hat{f}} \right) \left[ 2 + \sqrt{1-r^2} (\hat{f}_F^2 x^2 - r^2)^{-\frac{1}{2}} \right]}{\left[ \sqrt{1-r^2} (\hat{f}_F^2 x^2 - r^2)^{\frac{1}{2}} + (\hat{f}_F^2 x^2 - r^2) \right]^2} \\
& - \frac{4H_F \hat{f}_F^7 x^5 \sqrt{1-r^2} \left( \frac{x}{\hat{f}} + \frac{dx}{d\hat{f}} \right) \cdot (\hat{f}_F^2 x^2 - r^2)^{-\frac{3}{2}}}{\left[ \sqrt{1-r^2} (\hat{f}_F^2 x^2 - r^2)^{\frac{1}{2}} + (\hat{f}_F^2 x^2 - r^2) \right]^2} \\
& - \frac{8H_F \hat{f}_F^7 x^5 \left( \frac{x}{\hat{f}} + \frac{dx}{d\hat{f}} \right) \left[ 2 + \sqrt{1-r^2} (\hat{f}_F^2 x^2 - r^2)^{-\frac{1}{2}} \right]^2}{\left[ \sqrt{1-r^2} (\hat{f}_F^2 x^2 - r^2)^{\frac{1}{2}} + (\hat{f}_F^2 x^2 - r^2) \right]^3} \\
& - \frac{16H_F \hat{f}_F^5 x^3 \left( \frac{x}{\hat{f}} + \frac{dx}{d\hat{f}} \right) (3 - \hat{f}_F^2 x^2)}{(1 - \hat{f}_F^2 x^2)^3} \\
& - \frac{4H_F \hat{f}_F^3 x \left[ 3 \left( 3 \frac{x}{\hat{f}} + 2 \frac{dx}{d\hat{f}} \right) - \hat{f}_F^2 x^2 \left( 5 \frac{x}{\hat{f}} + 4 \frac{dx}{d\hat{f}} \right) \right]}{(1 - \hat{f}_F^2 x^2)^2} \left. \right\} \quad (A.20)
\end{aligned}$$

APPENDIX B  
PROGRAM FOR CALCULATING CHANNEL PARAMETERS





```

C      I = NI INDEX NUMBER FOR PATH
C      J = IF NUMBER OF HOPS
C      ZI REGION AND MAGNETOTOMIC INDICATOR (EO = E REGION =
      UNORDINARY WAVES) SIMILARLY FOR EX, FO, AND FX)
C      JI 'HIGH' (FOR HIGH RAY) OR 'LOW' (FOR LOW RAY)
C      NI SOLUTION INDICATOR (ANU SOLUTION, I= SOLUTION)
C      SI THETA = RAY ANGLE MEASURED FROM VERTICAL (DEGREES)
C      PI PATH LENGTH (KM)
C      FI DELAY AT CARRIER FREQUENCY (SEC)
C      BI RECEIVED CARRIER PHASE (CYCLES)
C      SI SIGNAL DELAY (SEC)
C      I0I AMPLITUDE DISTORTION (SEC/MHZ)
C      I1I PHASE DISTORTION (SEC/MHZ**2)
C      I2I ATTENUATION (DB)
C      I3I DOPPLER SHIFT (HZ)
C      I4I DOPPLER SPREAD (HZ)

PIWJ.1815926359
TMO'NITL'
PRT'PRT'
      READ DATA
      READ//,TL,BH
      READ//,XLONG,PLAT
      READ//,R
      READ//,RNG
      READ//,ISEA
      READ//,SPT
      READ//,ZEN
      READ//,SV09,TIME
      READ//,HEM,HE,FEU
      READ//,HFH,HF,FTU
      READ//,AS,SLT,SPMLT,SOLEXP
      READ//,SMIT,TEX,SMIB,SPROF,EXSPRT,RFH,RFQF
      READ//,SHIT,FXSHIT,SPRUF,FXSPRT,RFH,RFQF
      READ//,ZATTOIF
      READ//,GUELAY,UALIEM
      READ//,VOD,TPRINT
      READ//,PUNCH
      END READ DATA
C      COMPUTE PENETRATION FREQUENCIES FOR EXTRAORDINARY WAVES
C      CALL GETMAG(XLAT,XLONG,XIATH,XLONG)
      SINPHI=IN(PI/180.)*X(LATM)
      XHAT=XIATH*(16370./(16370.+HEM))**3
      FHEX=XHAT*(16370./(16370.+HEM))**3
      FPEX=XHAT*(16370./(16370.+HEM))**3
      FPEX=5*FHEX+SMIB*((FPEX**2)+(125*(FHEX**2)))
      FPEX=5*FHEX+SMIB*((FPEX**2)+(125*(FHEX**2)))
C      END COMPUTATION OF PENETRATION FREQS. FOR EXTRAORDINARY WAVES
C      COMPUTE BEARING OF RECEIVER IN MAGNETIC COORDINATES
      CALL RMAGMAG(XLAT,XLONG,M,RAG,RAM)
C      END COMPUTATION OF RECEIVER BEARING
      WRTF(6,910)
      WRTF(6,911)
      WRTF(6,912),FC,BW
      WRTF(6,913)
      WRTF(6,915),XLONG
      WRTF(6,916),PLAT
      WRTF(6,917),H

```

```

WRITE(6,918)MAG
WRITE(6,919)
WRITE(6,920)
WRITE(6,921)ISEA
WRITE(6,922)
WRITE(6,923)SPI
IF(CTIME-15.1M)GOTO9
WRITE(6,922)ZEN
GOTO10
9 WRITE(6,933)
10 IF(CTIME-15.1M)GOTO11
WRITE(6,924)
GOTO12
11 WRITE(6,925)
12 WRITE(6,926)HLM
SL=2.0HL
WRITE(6,927)SL
WRITE(6,928)FPEU
WRITE(6,930)FPLX
WRITE(6,929)HFM
SF=2.0HF
WRITE(6,927)SF
WRITE(6,928)FPEU
WRITE(6,930)FPLX
WRITE(6,953)
WRITE(6,954)HWSMTAPTHLT/SOLEXP
WRITE(6,945)
WRITE(6,946)SHIFTE/EXSHIF/SPROF/EXSPROF/REFREQ
WRITE(6,947)SHIFTE/EXSHIF/SPROF/EXSPROF/REFREQ
WRITE(6,900)
WRITE(6,934)
WRITE(6,900)
WRITE(6,935)GUELAY/RAFTEN
WRITE(6,936)
C DO 50 COMPUTES THE ARRAY T(I,J)
NUGONHOP=126
NHUP=FLDAT(NHUP)
RHER/XNHOP
NHUP=8*(NHUP-1)
DUTSTRT=8
I=1+NHOP
T(I,I)=NHOP
35 CONTINUE
T(I+1,NHOP)
C ASSIGN LABELS TO EACH TRANSMISSION MODE
T(I,2)=1E0
T(I,3)=1E0M
T(I,4)=1E0
T(I,2)=1E0
T(I,3)=1E0HIGH
T(I,4)=1E0
T(I,2)=1E0
T(I,3)=1E0M
T(I,4)=1E0
T(I,2)=1E0
T(I,3)=1E0HIGH
T(I,4)=1E0
T(I,2)=1E0
T(I,3)=1E0M
T(I,4)=1E0

```



```

T(1,2)=EX'
T(1,3)=HIGH'
I=1
T(1,2)=EX'
T(1,3)=LOW'
I=1
T(1,2)=EX'
T(1,3)=HIGH'
END LABFL ASSIGNMENT
NMAG = 1 FOR ORDINARY WAVES NMAG = 2 FOR EXTRAORDINARY WAVE
DO 36 NMAG=1,2
IF (NMAG=1) 36, 36, 37
SUBROUTINE PATH' RETURNS ARRAY P(I,J) CONTAINING SIGNAL
PATH LENGTHS DELAY AND DELAY DERIVATIVES
36 CALL PATH(MH,FEU,FFD,FC,P)
GU036
37 CALL PATH(RH,FEH,FEF,FC,P)
38 DO 40 I=1,4
I=1+4*(NMAG-1)+NMHOP
T(1,4)=P(I,1)
T(1,5)=(180./PI)*ARCOS(P(I,3))*P(I,1)
T(1,6)=XNHOP*P(I,4)
T(1,7)=P(I,5)*XNHOP
T(1,8)=FC*P(I,5)*XNHOP/I*(E+06)
INT=1(I,8)
T(1,8)=T(1,8)+INT
T(1,9)=P(I,6)*FC*P(I,6)*XNHOP
T(1,10)=P(I,6)*5*FC*P(I,7)*XNHOP
T(1,11)=((5*P(I,7))*FC*P(I,6))/6.*XNHOP
C COMPUTE ATTENUATION
XND=P(I,1)*(1.E-08)
T(1,12)=21*20
TH=1(I,15)
DIST=T(1,8)
XAG=3.-2*FLUAT(NMAG)
AC1=WARSMLT
AC2=SPIMLT
AC3=SQEXP
CALL ATEN(XLAIM,TH,RAH,SP,LEN,TIME,DIS,XNHOP,FL,XMAG,A,ATT)
T(1,12)=ATT
GU022
71 T(1,12)=0
C F.N. COMPUTATION OF ATTENUATION
C COMPUTE DOPPLER SHIFTS AND SPREADS
72 XND=FLJAI(1)-2*5
JFXTNDJ2J2J2J24
73 T(1,13)=XNHOP*SHIFTE*((FC/HFREWE)*XSHTE)*P(I,1)
T(1,14)=SQRT(XNHOP)*SPHNF*((FC/HFREWE)*EXSPH)*P(I,1)
GU025
74 T(1,13)=XNHOP*SHIFTE*((FC/HFREWE)*XSHIF)*P(I,1)
T(1,14)=SQRT(XND)*SPHNF*((FC/HFREWE)*EXSPH)*P(I,1)
75 CONTINUE
C END COMPUTATION OF SHIFTS AND SPREADS
80 CONTINUE
90 CONTINUE
C NO 70 DETERMINES MINIMUM (MINZERU) ATTENUATION
ATTMIN=L*05
ATTMAX=L*40
DO 70 I=1,40

```



5000 51 813

909 FORMAT(6X,'SUMMARY OF TRANSMISSION PARAMETERS',//)  
 910 FORMAT(1X,'SIGNAL PARAMETERS',//)  
 911 FORMAT(1X,'CARRIER FREQ. =',F7.3,' MHz. BANDWIDTH =',F7.2,' MHz  
 1.//)  
 912 FORMAT(1X,'TRANSMITTER/RECEIVER PARAMETERS',//)  
 913 FORMAT(1X,'LOCATION OF TRANSMITTER LONGITUDE =',F7.2,' DEGREES (E  
 1.// FOR WEST, - FOR EAST)',//)  
 914 FORMAT(1X,'LATITUDE =',F7.2,' DEGREES (+ FOR NORTH, - FOR SOUTH  
 1.//)  
 915 FORMAT(1X,'DISTANCE BETWEEN TRANSMITTER AND RECEIVER =',F6.2,' KM.  
 1.//)  
 916 FORMAT(1X,'DIRECTION FROM TRANSMITTER TO RECEIVER =',F6.2,' DEGREE  
 1.//)  
 917 FORMAT(1X,'TRANSMITTER ANTENNA PATTERN = (3/2)\*(SIN(THETA))<sup>2</sup>',//)  
 918 FORMAT(1X,'RECEIVER ANTENNA PATTERN = (3/2)\*(SIN(THETA))<sup>2</sup>',//)  
 919 FORMAT(1X,'SEA STATE =',F7.2//)  
 920 FORMAT(1X,'IONOSPHERE PARAMETERS',//)  
 921 FORMAT(1X,'SUNSPOT NUMBER =',F7.2//)  
 922 FORMAT(1X,'DAYTIME ELECTRON DENSITY PROFILE',//)  
 923 FORMAT(1X,'NIGHTTIME ELECTRON DENSITY PROFILE',//)  
 924 FORMAT(1X,'REGIONAL HEIGHT OF MAX. ELECTRON DENSITY =',F7.2,' KM  
 1.//)  
 925 FORMAT(1X,'PENETRATION FREQUENCY, EXTRAORDINARY WAVE =',F7.3,' MHz  
 1.//)  
 926 FORMAT(1X,'SOLAR ZENITH ANGLE =',F7.2,' DEGREES',//)  
 927 FORMAT(1X,'SOLAR ZENITH ANGLE = NOT APPLICABLE TO NIGHTTIME TRANSM  
 1.//)  
 928 FORMAT(1X,'COMPUTED CHANNEL PARAMETERS',//)  
 929 FORMAT(1X,'GROUNDWAVE DELAY =',F10.3,' SEC. ATTENUATION =  
 1.// F10.3, ' dB',//)  
 930 FORMAT(1X,'IONOSPHERE RETURN',//)  
 931 FORMAT(1X,'CARRIER',//)  
 932 FORMAT(1X,'SIGNAL',//)  
 933 FORMAT(1X,'UPPER',//)  
 934 FORMAT(1X,'DOWN',//)  
 935 FORMAT(1X,'DISTORTION',//)  
 936 FORMAT(1X,'SPREAD',//)  
 937 FORMAT(1X,'SOLN',//)  
 938 FORMAT(1X,'SEC/MHZ',//)  
 939 FORMAT(1X,'F10.3',//)  
 940 FORMAT(1X,'F10.3',//)  
 941 FORMAT(1X,'F10.3',//)  
 942 FORMAT(1X,'F10.3',//)  
 943 FORMAT(1X,'F10.3',//)  
 944 FORMAT(1X,'F10.3',//)  
 945 FORMAT(1X,'F10.3',//)  
 946 FORMAT(1X,'F10.3',//)  
 947 FORMAT(1X,'F10.3',//)  
 948 FORMAT(1X,'F10.3',//)  
 949 FORMAT(1X,'F10.3',//)  
 950 FORMAT(1X,'F10.3',//)  
 951 FORMAT(1X,'F10.3',//)  
 952 FORMAT(1X,'F10.3',//)  
 953 FORMAT(1X,'F10.3',//)  
 954 FORMAT(1X,'F10.3',//)  
 955 FORMAT(1X,'F10.3',//)  
 956 FORMAT(1X,'F10.3',//)  
 957 FORMAT(1X,'F10.3',//)  
 958 FORMAT(1X,'F10.3',//)  
 959 FORMAT(1X,'F10.3',//)  
 960 FORMAT(1X,'F10.3',//)  
 961 FORMAT(1X,'F10.3',//)  
 962 FORMAT(1X,'F10.3',//)  
 963 FORMAT(1X,'F10.3',//)  
 964 FORMAT(1X,'F10.3',//)  
 965 FORMAT(1X,'F10.3',//)  
 966 FORMAT(1X,'F10.3',//)  
 967 FORMAT(1X,'F10.3',//)  
 968 FORMAT(1X,'F10.3',//)  
 969 FORMAT(1X,'F10.3',//)  
 970 FORMAT(1X,'F10.3',//)  
 971 FORMAT(1X,'F10.3',//)  
 972 FORMAT(1X,'F10.3',//)  
 973 FORMAT(1X,'F10.3',//)  
 974 FORMAT(1X,'F10.3',//)  
 975 FORMAT(1X,'F10.3',//)  
 976 FORMAT(1X,'F10.3',//)  
 977 FORMAT(1X,'F10.3',//)  
 978 FORMAT(1X,'F10.3',//)  
 979 FORMAT(1X,'F10.3',//)  
 980 FORMAT(1X,'F10.3',//)  
 981 FORMAT(1X,'F10.3',//)  
 982 FORMAT(1X,'F10.3',//)  
 983 FORMAT(1X,'F10.3',//)  
 984 FORMAT(1X,'F10.3',//)  
 985 FORMAT(1X,'F10.3',//)  
 986 FORMAT(1X,'F10.3',//)  
 987 FORMAT(1X,'F10.3',//)  
 988 FORMAT(1X,'F10.3',//)  
 989 FORMAT(1X,'F10.3',//)  
 990 FORMAT(1X,'F10.3',//)  
 991 FORMAT(1X,'F10.3',//)  
 992 FORMAT(1X,'F10.3',//)  
 993 FORMAT(1X,'F10.3',//)  
 994 FORMAT(1X,'F10.3',//)  
 995 FORMAT(1X,'F10.3',//)  
 996 FORMAT(1X,'F10.3',//)  
 997 FORMAT(1X,'F10.3',//)  
 998 FORMAT(1X,'F10.3',//)  
 999 FORMAT(1X,'F10.3',//)  
 1000 FORMAT(1X,'F10.3',//)

954	FORMAT(15X,'MULTIPLICATIVE CONSTANT =',F6.2,'',SUNSPOT NUMBER MULT	L	0021034113
	1PL1TR =',F6.6,'',SOLAR ZENITH ANGLE EXPONENT =',F6.3)	L	0021034113
955	FORMAT(11A2,A4,4E16.9)	L	0021034113
956	FORMAT(4E16.9)	L	0021034113
957	FORMAT(4E16.9)	L	0021034113
	SIN	L	0021034113
	PAN	L	0021035012
	0021035213 IS THE LOCATION FOR EXCEPTIONAL ACTION ON THE I/O STATEMENT AT 002100AD		
	0021035215 IS THE LOCATION FOR EXCEPTIONAL ACTION ON THE I/O STATEMENT AT 002100VC		
	0021035217 IS THE LOCATION FOR EXCEPTIONAL ACTION ON THE I/O STATEMENT AT 0021009A		
	0021035219 IS THE LOCATION FOR EXCEPTIONAL ACTION ON THE I/O STATEMENT AT 0021008A		
	002103521B IS THE LOCATION FOR EXCEPTIONAL ACTION ON THE I/O STATEMENT AT 0021007A		
	002103521C IS THE LOCATION FOR EXCEPTIONAL ACTION ON THE I/O STATEMENT AT 0021006B		
	002103521D IS THE LOCATION FOR EXCEPTIONAL ACTION ON THE I/O STATEMENT AT 0021005A		
	002103521E IS THE LOCATION FOR EXCEPTIONAL ACTION ON THE I/O STATEMENT AT 0021004D		
	002103521F IS THE LOCATION FOR EXCEPTIONAL ACTION ON THE I/O STATEMENT AT 0021003D		
	002103521G IS THE LOCATION FOR EXCEPTIONAL ACTION ON THE I/O STATEMENT AT 00210035		
	002103521H IS THE LOCATION FOR EXCEPTIONAL ACTION ON THE I/O STATEMENT AT 0021002D		
	0021036211 IS THE LOCATION FOR EXCEPTIONAL ACTION ON THE I/O STATEMENT AT 00210025		
	0021036213 IS THE LOCATION FOR EXCEPTIONAL ACTION ON THE I/O STATEMENT AT 0021001D		
	0021036215 IS THE LOCATION FOR EXCEPTIONAL ACTION ON THE I/O STATEMENT AT 00210013		
	0021036217 IS THE LOCATION FOR EXCEPTIONAL ACTION ON THE I/O STATEMENT AT 00210009		

SECRET 002 IS 03CF LUNG



	SUBROUTINE BNGHAG(PHIT,XLAMT,PARGLE,ANGLEM)	START OF SEGMENT 00B
C		C 00B1000010
C	SUBROUTINE COMPUTES BEARING OF THE RECEIVER FROM THE	C 00B1000010
C	TRANSMITTER IN MAGNETIC COORDINATES	C 00B1000010
C	PHIT = GEOMAGNETIC LATITUDE OF TRANSMITTER (DEGREES)	C 00B1000010
C	XLAMT = GEOMAGNETIC LONGITUDE OF TRANSMITTER (DEGREES)	C 00B1000010
C	N = DISTANCE BETWEEN TRANSMITTER AND RECEIVER (KM)	C 00B1000010
C	ANGLEM = BEARING OF RECEIVER IN GEOGRAPHIC COORDINATES (DEGREES)	C 00B1000010
C	ANGLEM = BEARING OF RECEIVER IN MAGNETIC COORDINATES (DEGREES)	C 00B1000010
		C 00B1000010
		C 00B1000010
		C 00B1000010
		C 00B1000010
5	PHIT=PHIT*(PI/180.0)	C 00B1000011
	GOTO 6	C 00B1000014
6	IF (G=1.0) G=1.0	C 00B1000011
7	PHIT=PHIT*(PI/180.0)	C 00B1000012
8	XLAMT=XLAMT*(PI/180.0)	C 00B1000015
	GOTO 10	C 00B1000014
10	ANGLEM=ANGLEM*(PI/180.0)	C 00B1000011
	W=PI/4.0	C 00B1000010
	GE=CC*ANGLEM/72.0	C 00B1000013
	U1=(A-B)/2.0	C 00B1000012
	S1=(A+B)/2.0	C 00B1000011
	W1=SIN(U1)/(TAN(Q)*SIN(S1))	C 00B1000010
	W2=COS(U1)/(TAN(Q)*COS(S1))	C 00B1000015
	Z1=TAN(W1)	C 00B1000014
	Z2=TAN(W2)	C 00B1000011
	W3=(TAN(S1)*COS(Z2))/COS(Z1)	C 00B1000014
	W4=TAN(W3)	C 00B1000013
	PHI=90.0-(C/CL)	C 00B1000013
	XLAMT=XLAMT*(PI/180.0)	C 00B1000012
20	CALL GEOMAG(PHIT,XLAMT,PHITM,XLAMTM)	C 00B1000014
	CALL GEOMAG(PHIT,XLAMT,PHITM,XLAMTM)	C 00B1000012
	N2=CC/4.0*(PHITM-PHIT)	C 00B1000010
	S2=CC/2.0*(PHITM-PHIT)	C 00B1000012
	D=(CC/2.0)*(XLAMTM-XLAMT)	C 00B1000014
	IF (D>50.0) D=50.0	C 00B1000010
30	IF (PHITM-PHIT)>51.52+52	C 00B1000015
31	ANGLEM=180.0	C 00B1000011
	GOTO 100	C 00B1000010
32	ANGLEM=0.0	C 00B1000013
	GOTO 100	C 00B1000011
33	W5=CC/2.0*(TAN(D)*COS(S2))	C 00B1000014
	W6=CC/2.0*(TAN(D)*SIN(S2))	C 00B1000012
	Z3=TAN(W5)	C 00B1000015
	Z4=TAN(W6)	C 00B1000012
100	RETURN	C 00B1000015
	END	C 00B1000012
	SEGMENT 00B IS 005C LONG	



C	SUBROUTINE GETLUM(PHIG,XI ANG,PHIM,XLANG)		START OF SEGMENT UOF
C	PHIG = GEOGRAPHIC LATITUDE (DEGREES)	L	OOF1000010
C	XLANG = GEOGRAPHIC LONGITUDE (DEGREES)	L	OOF1000010
C	PHIM = MAGNETIC LATITUDE (DEGREES)	L	OOF1000010
C	XLANG = MAGNETIC LONGITUDE (DEGREES)	L	OOF1000010
C	PIC=1015726559	L	OOF1000010
C	CP1/1804	L	OOF1000510
C	A1=COPHIG	L	OOF1000010
C	A2=CXLANG	L	OOF1000010
C	A3=CX78.3	L	OOF1000012
C	A4=C69.	L	OOF1000014
C	R1=STN(A1)*SIN(A3)+COS(A1)*COS(A3)*COS(A2-AR)	L	OOF1000010
C	PHIMARSIN(B1)	L	OOF1001214
C	R2=(COS(A1)*SIN(A2-A4))/COS(PHIM)	L	OOF1001411
C	PHIMPHIM/C	L	OOF1001013
C	XLANG=AKSIN(R2)/C	L	OOF1001415
C	PUTUN	L	OOF1001315
C	END	L	OOF1001112
			SEGMENT OUF IS 0020 LUNG

[illegible]



```

30  CONTINUL
C      IF MIN, AL(X) .GT. P, THERE ARE NO RETURNS FROM E REGION
      IF (AMIN-R)40,40,31
11  00350=1.0
      P(1,0)=0.
      P(2,0)=0.
35  CONTINUL
      00700
C      DO 50 DETERMINE X = CUS(THETA) FOR E REGION LOW RAY
40  XLAST=1.E=10
      00500=1.0
      DIFF=1.-(10.**L)
46  X=XLAST-DIFF
      IF (X-AMIN)47,49,49
47  CALL AELFPEF(X,A)
      IF (A-R)59,49,48
48  XLAST=X
      00700
49  XLAST=X-DIFF
50  CONTINUE
      P(1,0)=1.
      P(1,2)=2.
      X=AMIN(X,1.)
      P(1,2)=X
      P(1,0)=X/SORT(1.-X**2)
      CALL DELAYE(R,FPEF,X,T,0.1T,0.2T,0.3T)
      P(1,5)=1.
      P(1,2)=1
      P(1,7)=0.2T
      P(1,8)=0.3T
      IF (FNE-1.)200,200,60
C      DO 70 DETERMINE X = CUS(THETA) FOR E REGION HIGH RAY
40  XLAST=(1./FNF)-1.E=10
      00700=1.0
      DIFF=1.-(10.**L)
46  X=XLAST-DIFF
      IF (X-AMIN)69,69,67
47  CALL AELFPEF(X,A)
      IF (A-R)69,69,68
48  XLAST=X
      00700
49  XLAST=X-DIFF
70  CONTINUE
      P(2,0)=1.
      P(2,2)=2.
      X=AMIN(X,1.)
      P(2,2)=X
      P(2,0)=X/SORT(1.-X**2)
      CALL DELAYE(H,FPEF,X,T,0.1T,0.2T,0.3T)
      P(2,5)=1
      P(2,6)=0.1T
      P(2,7)=0.2T
      P(2,8)=0.3T
40  IF (FNF-1.)90,90,100

```



```

90      X4TM=1.
      D95J=1.8
      P(4,2)=0.
95      CONTINUE
      GOTO120
C
      DO 110 DETERMINES MINIMUM VALUE OF AF(X)
100      XLAST=(1./FNF)+1.E-11
      CALL AF(FPE,FPP,F,ALAST,ALAST)
      D0110L=1.10
      DIFF=1./((10.*AL)
104      XMIN=XLAST+DIFF
      IF(FNF*XMIN=1.)107,109,109
107      CALL AF(FPE,FPP,F,XMIN,XMIN)
      IF(XMIN=ALAST)100,109,100
108      XLAST=XMIN
      ALAST=XMIN
      GOTO106
109      IF(C=1)116,116,117
116      XLAST=XMIN+DIFF
      GOTO118
117      XLAST=XMIN+2.*DIFF
118      CALL AF(FPE,FPP,F,ALAST,ALAST)
110      CONTINUE
C
      IF MIN. AF(X) .GT. 0. THERE ARE NO RETURNS FROM F REGION
111      IF(XMIN=120)120,120,111
      D0115J=1.8
      P(3,2)=0.
      P(4,2)=0.
115      CONTINUE
      GOTO200
C
      DO 130 DETERMINES X = COS(THETA) FOR F REGION LOW MAY
120      XLAST=(1./FNF)+1.E-11
      D0130L=1.9
      DIFF=1./((10.*AL)
124      X=XLAST+DIFF
      IF(X=XMIN)127,129,129
127      CALL AF(FPE,FPP,F,X,A)
      IF(A-R)129,129,128
128      XLAST=X
      GOTO126
129      XLAST=X+DIFF
130      CONTINUE
      P(3,2)=0.
      P(3,2)=0.
      X=XMIN+(X-1.)
      P(3,2)=0.
      P(3,2)=0.
      CALL DELTA(FPE,FPP,F,X,Y,DT,DT,M3Y)
      P(3,2)=0.
      P(3,2)=0.
      P(3,2)=0.
      IF(FNF=1.)200,200,140

```

```

C      DO 150 N=1,NM1,X = COS(THETA) FOR F REGION HIGH RAY
140  X1=AST*(1./FNF)-1./E-11
    OUTSOL=1210
    DIFF=1./C10.*e1.)
146  Y=LAST-DIFF
    T1(X=XMIN)149,149,147
147  CALL AF(FPE,FPA,F,X,A)
    T1(A=R)149,149,146
148  XLAST=X
    GOTU146
149  XLAST=X+DIFF
150  CUNT=146
    P147)=1.
    P148)=2.*M
    X=ATN(C10/X1)
    P149)=X
    P148)=R/SQRT(1.-X**2)
    CALL DELATF(M,P147,P148,P149,T,01T,02T,03T)
    P145)=1
    P146)=01T
    P147)=02T
    P148)=03T
    P149)=04T
150  RETURN
    END

```

B-14









B-18



APPENDIX C  
COMPUTER GENERATION OF RANDOM GAINS



APPENDIX C  
COMPUTER GENERATION OF RANDOM GAINS

For each ionosphere return, it is desired to generate a stationary, zero-mean Gaussian sequence  $\hat{G}_j(nT_0)$ ,  $n = 0, 1, \dots$ , having the correlation function

$$\begin{aligned} C_{\hat{G}_j}(nT_0) &= E \hat{G}_j(nT_0 + mT_0) \hat{G}_j^*(mT_0) \\ &= A_j^2 \left[ 1 + (2\pi\rho\sigma_j T_0 |n|) + \frac{1}{3} (2\pi\rho\sigma_j T_0 |n|)^2 \right] \\ &\quad \cdot \exp \left[ -2\pi\rho\sigma_j T_0 |n| + 2\pi i v_j T_0 n \right] \end{aligned} \quad (C.1)$$

$$n = 0, 1, \dots$$

$$j = 1, \dots, N.$$

We will generate this sequence by passing a white noise process through an appropriately chosen discrete-time linear filter [26]. Denoting the filter input by  $\{\xi_j(n)\}$  and the impulse response by  $\{a_j(n)\}$  we have

$$\hat{G}_j(nT_0) = \exp[2\pi i v_j n T_0] \sum_{m=0}^{\infty} \xi_j(n-m) a_j(m) \quad (C.2)$$

$j=1, \dots, N$

where

$$a_j(m) = \begin{cases} A_j \left( \frac{8}{3} \pi \rho \sigma_j T_0 \right)^{\frac{1}{2}} (2\pi \rho \sigma_j m T_0)^2 \exp \left[ -2\pi \rho \sigma_j m T_0 \right], & m \geq 0 \\ 0, & m < 0 \end{cases}, \quad j=1, \dots, N. \quad (C.3)$$

The random variables  $\{\xi_j(n)\}$  are independent, identically-distributed, complex Gaussian variables. They may be expressed as

$$\xi_j(n) = \xi_j^{(1)}(n) + i\xi_j^{(2)}(n) \quad , \quad n=0,1,\dots \quad (C.4)$$

where  $\xi_j^{(1)}(n)$  and  $\xi_j^{(2)}(n)$  are, respectively, the real and imaginary parts of  $\xi_j(n)$ . For each  $n$  the variables  $\xi_j^{(1)}(n)$  and  $\xi_j^{(2)}(n)$  are independent, zero-mean, unit variance, real Gaussian variables, and both components of  $\xi_j(n)$  are independent of each other for all values of  $n$ .

To generate  $\tilde{G}_j(nT_0)$  directly using the convolution (C.2), we would have to approximate the infinite summation with a sufficiently accurate truncated summation. Because  $\sigma_j T_0$  is very small, the length of this truncated summation would be large and we would expect error accumulation and an attendant loss of accuracy. However, our particular choice of an approximating correlation function (C.1) allows us to generate the random sequence  $G_j(nT_0)$  iteratively. This was, of course, the primary consideration in selecting this particular approximation. The iterative scheme is given below

$$\begin{aligned} \tilde{G}_j(nT_0 + 3T_0) = & K_j \exp[-2\pi\rho\sigma_j T_0 + 2\pi i v_j(n+3)T_0] \xi_j(n+2) \\ & + K_j \exp[-4\pi\rho\sigma_j T_0 + 2\pi i v_j(n+3)T_0] \xi_j(n+1) \\ & + \exp[-6\pi\rho\sigma_j T_0 + 6\pi i v_j T_0] \tilde{G}_j(nT_0) \\ & - 3 \exp[-4\pi\rho\sigma_j T_0 + 4\pi i v_j T_0] \tilde{G}_j(nT_0 + T_0) \\ & + 3 \exp[-2\pi\rho\sigma_j T_0 + 2\pi i v_j T_0] \tilde{G}_j(nT_0 + 2T_0) \end{aligned} \quad (C.5)$$

$n \geq 0$   
 $j=1, \dots, N$

where

$$K_j = \frac{2}{\sqrt{3}} A_j (2\pi\rho\sigma_j T_o)^{\frac{5}{2}}, \quad j=1, \dots, N \quad (C.6)$$

and, as discussed earlier, we will choose  $\rho = 2.1$ . To start this iteration we need  $\tilde{G}_j(0)$ ,  $\tilde{G}_j(T_o)$  and  $\tilde{G}_j(2T_o)$  given by

$$\tilde{G}_j(0) = A_j W_j(1) \quad (C.7)$$

$$\tilde{G}_j(T_o) = \exp[2\pi i \nu_j T_o] \cdot \gamma_j(1) W_j(2) + \lambda_j(1) \tilde{G}_j(0) \quad (C.8)$$

$$\begin{aligned} \tilde{G}_j(2T_o) = \exp[4\pi i \nu_j T_o] \cdot \{ \gamma_j(2) W_j(3) + K_j \exp[-2\pi\rho\sigma_j T_o] \xi_j(1) \\ + \lambda_j(1) [1 - \lambda_j(2)] \tilde{G}_j(T_o) + \lambda_j(2) \tilde{G}_j(0) \} \end{aligned} \quad (C.9)$$

$$j=1, \dots, N.$$

Here  $W_j(1)$ ,  $W_j(2)$ ,  $W_j(3)$ , and  $\xi_j(1)$  are independent, complex, Gaussian variables whose real and imaginary parts are independent and have zero mean and unit variance. The other terms appearing in (C.7)-(C.9) are

$$\lambda_j(1) = [1 + (4\pi\rho\sigma_j T_o) + \frac{1}{3} (4\pi\rho\sigma_j T_o)^2] \cdot \exp[-4\pi\rho\sigma_j T_o] \quad (C.10)$$

$$\lambda_j(2) = [1 + (8\pi\rho\sigma_j T_o) + \frac{1}{3} (8\pi\rho\sigma_j T_o)^2] \cdot \exp[-8\pi\rho\sigma_j T_o] \quad (C.11)$$

$$\gamma_j(1) = A_j [1 - \lambda_j^2(1)]^{\frac{1}{2}} \quad (C.12)$$

$$\gamma_j(2) = A_j \left[ \left(1 - \lambda_j^2(1)\right) \left(1 - \lambda_j^2(2)\right) - \frac{4}{3} \left(2\pi\rho\sigma_j T_o\right)^5 \exp[-4\pi\rho\sigma_j T_o] \right]^{\frac{1}{2}} \quad (C.13)$$

The coefficients  $A_j$  are determined by the attenuation of each return via Eqn. (43).

It remains to generate the sequence of independent, Gaussian variables  $\{\xi_j(n)\}$ . We begin by using the congruence method to generate a sequence of uniform random variables. This method generates a sequence of random integers via the iterative scheme [24]

$$Y_{n+1} = a \cdot Y_n \pmod{M} . \quad (C.14)$$

For the quantities  $a$  and  $M$ , we have found  $a = 7^5$  and  $M = 2^{31}$  to be effective. Multiplication is done using double precision arithmetic but the final result is expressed as a single precision variable. Upon division of  $\{Y_n\}$  by  $2^{31}$  a sequence of independent, uniform  $[0,1]$  variables is produced. This sequence is then transformed into a sequence of independent, complex, Gaussian variables. If  $u_1$  and  $u_2$  are real, independent, uniform variables, the real and imaginary parts of the variable  $\xi$  defined by

$$\xi = (-2 \ln u_1)^{1/2} \exp[2\pi i u_2] \quad (C.15)$$

are independent and Gaussian with zero mean and unit variance [24]. Thus, we obtain the desired sequence of complex Gaussian variables for use as the filter input in Eqn. (C.5).



APPENDIX D  
SIGNAL ANALYSIS PROGRAM

86700/97700 F D W T R A N C D M P I L A T I O N M A R K 2.0.060 MONDAY, 09/26/71 02:22 PM

FILE 2(KIND=TAPE, TITLE='HFOUTPUT')  
FILE 10(KIND=TAPE, TITLE='HFINPUT')

START OF SEGMENT 002  
FORMAT SEGMENT IS OCV LONG  
FORMAT SEGMENT IS OCV LONG

DIMENSION T(10,14),D2(10),D3(10),M(10)  
COMPLEX X(10,4),Y(10,4),Z(10),D(10),B(10),S(10),A(10)  
COMPLEX PR(10000),QR(10000),SI(10000)  
DOUBLE PRECISION C(10,7)

C THIS PROGRAM IS THE SIGNAL ANALYSIS PART OF THE SIMULATOR

C FC = CARRIER FREQUENCY (MHZ)  
C BW = BANDWIDTH (MHZ)  
C RANGE = DISTANCE BETWEEN TRANSMITTER AND RECEIVER (KM.)  
C TIME = TIME OF DAY ('DAY' OR 'NITE')  
C NPATH = NUMBER OF RETAINED IONOSPHERE RETURNS  
C NUMIN = NUMBER OF INPUT SAMPLES  
C NTAPE = TAPE WRITE SELECTOR (WRITES TAPE IF NTAPE=1)  
C NGAIN = RANDOM GAIN SELECTOR (MULTIPLIES BY RANDOM GAINS ONLY IF NGAIN=1)  
C NPRTM = NUMBER OF OUTPUT VALUES TO BE PRINTED  
C NGAINV = ONE-SIDED LENGTH OF TRUNCATED IMPULSE RESPONSE  
C GDLAY = GROUNDWAVE DELAY (SEC.)  
C GATTN = GROUNDWAVE ATTENUATION (DB)  
C ALPHA = PARAMETER USED IN APPROXIMATE SPECTRUM  
C NGND = GROUNDWAVE DELAY SHIFT PARAMETER  
C ISEED = SEED VALUE USED IN RANDOM NUMBER GENERATOR, IT IS SET = 7\*5 FOR FIRST CALL AND IT IS REPLACED BY A NEW VALUE TO BE USED IN SUBSEQUENT CALLS  
C NMIN = MINIMUM DELAY SHIFT PARAMETER  
C NMAX = MAXIMUM DELAY SHIFT PARAMETER  
C GNDUJ = DELAYED, ATTENUATED GROUNDWAVE  
C SIGOUT = OUTPUT SIGNAL (GROUNDWAVE+IONOSPHERE RETURNS)  
C THE ARRAY D(10) CONTAINS TERMS IN IMPULSE RESPONSE, IT IS PRODUCED BY THE SUBROUTINE 'IMPULS'.

C THE ARRAY D2(10) CONTAINS AMPLITUDE DISTORTION COEFFICIENTS  
C THE ARRAY D3(10) CONTAINS PHASE DISTORTION COEFFICIENTS  
C THE ARRAY M(10) CONTAINS SIGNAL DELAY SHIFT PARAMETERS  
C THE ARRAY S(10000) CONTAINS INPUT SIGNAL SEQUENCE

C THE ARRAY C(10,7) CONTAINS THE RANDOM GAINS, IT IS PRODUCED BY THE SUBROUTINE 'GAIN'.

C THE ARRAYS C(10,7), Y(10,4) AND Z(10) CONTAIN VARIABLES USED IN SUBROUTINE 'GAIN', THEY ARE SET = 0 FOR FIRST CALL.

C THE ARRAY T(10,14) CONTAINS THE IONOSPHERE CHANNEL PARAMETERS, ITS ENTRIES ARE:

C I = INDEX NUMBER FOR PATH  
C J = 11 NUMBER OF HOPS  
C K = 21 REGION AND MAGNETOTONIC INDICATOR (ED = E REGION - ORDINARY WAVES SIMILARLY FOR EX, F, AND FX)  
C L = 31 'HIGH' (FOR HIGH RAY) OR 'LOW' (FOR LOW RAY)  
C M = 41 SOLUTION INDICATOR (0=NO SOLUTION, 1= SOLUTION)  
C N = 51 THETA = RAY ANGLE MEASURED FROM VERTICAL (DEGREES)





```

C      INITIALIZE ARRAYS FOR CONVOLUTION
      DOUT=1,NPATH
      D2(1)=1,10,2,2,PI*(RM+2)
      D3(1)=1,1,1,1,2,2,PI*(RM+3)*(1-E*03)
      NM=ABS(T(1,0))/10
      XM=10-10*FLOAT(NM)
      IF(T(1,0))32,34,34
32  NM2=-1
      GOTO36
34  NM2=1
36  IF(NM)5,38,38,39
38  N1(1)=N1+NM2
      GOTO40
39  N1(1)=N1+1,NN2
40  CONTINUE
C      END INITIALIZATION OF ARRAYS FOR CONVOLUTION
      DETERMINE NONG
      NG1=GOENAY/10
      XS=10-10*FLOAT(NG1)
      IF(NG1)5,42,42,44
42  NGND=NG1
      GOTO45
44  NGND=NG1+1
C      END DETERMINATION OF NGND
C      DETERMINE MAX. AND MIN. DELAY SHIFT PARAMETERS
45  LLIMIT=2*NCNVL+1
      NIMAX=NGND
      NIMIN=NGND
      DOUT=1,NPATH
      NIMAX=XO(NIMAX,MIT)
      NIMIN=XO(NIMIN,MAC)
      NIMIN=MIN(NIMIN,MAC)
48  CONTINUE
C      END DETERMINATION OF MAX. AND MIN. SHIFT PARAMETERS
C      READ INITIAL INPUT SEQUENCE
      MHEAD=NIMAX-NIMIN+LLIMIT
      MHEAD=MHEAD-1
      IF(NHEAD)50,150,50,55
45  WHIF(16,903)
      GOTO99
50  DOUT=1,NHEAD
      XLL=FLUAT(L-1)
      READ(10,904)SIGIN(L)
40  CONTINUE
C      END READ INITIAL INPUT SEQUENCE
      NSHIFT=0
      CALL IMPULS(NCNVL,NPATH,D2,D3,D)
C      D2=DOUN1,NM,NM
      DETERMINE DISTORTED THERMOSPHERE RETURNS
      DOUT=1,NPATH
      RCT=(0,0,0)
70  CONTINUE
      DOUT=1,LLIMIT
      L=2,NCNVL+1,2
      L=L-NCNVL+1,NSHIFT+1
      DOUT=1,NPATH
      L=L-N1(1)

```



D-4



```

924  FORMAT(1X,'THE FOLLOWING DATA REPRESENTS THE RECEIVED, COMPLEX GAS
    1EBAND SIGNAL. IT INCLUDES THE GROUNDWAVE AND ALL IONOSPHERE RETURN
    2S.'/)
930  FORMAT(1X)
934  FORMAT(1X,'COMPUTER CHANNEL PARAMETERS')
935  FORMAT(1X,'GROUNDWAVE DELAY =',F10.3,' SEC. ATTENUATION =',
    1,'F10.3,' DB.')
936  FORMAT(1X,'IONOSPHERE RETURN')
938  FORMAT(1X,'MODE',3X,'SOLUTION',3X,'RAY ANGLE',3X,'PATH',3X,'CARRI
    1ER',3X,'CARRIER',3X,'SIGNAL',3X,'AMPLITUDE',3X,'PHASE',5X,'ATT
    2ENUATION',2X,'DUPPER',4X,'DUPPLER')
939  FORMAT(10X,'INTEGRATION',2X,'(DEGREES)',2X,'LENGTH',3X,'DELAY',6X,'P
    1ASE',6X,'DELAY',3X,'DISTORTION',1X,'DISTORTION',3X,'(DB)',7X,'S
    2HIFT',5X,'SPREAD')
940  FORMAT(9X,'(UNNU SOLN)',13X,'(KN)',3X,'(SEC)',3X,'(CYCLES)',5X,'(
    1SEC)',3X,'(SEC/MHZ)',1X,'(SEC/MHZ)',15X,'(HZ)',7X,'(HZ)')
951  FORMAT(1X,'A2',1X,'A4',1X,'A6',1X,'A8',1X,'A10',1X,'A12',1X,'A14',1X,'A16',1X,'A18',1X,'A20',1X,'A22',1X,'A24',1X,'A26',1X,'A28',1X,'A30',1X,'A32',1X,'A34',1X,'A36',1X,'A38',1X,'A40',1X,'A42',1X,'A44',1X,'A46',1X,'A48',1X,'A50',1X,'A52',1X,'A54',1X,'A56',1X,'A58',1X,'A60',1X,'A62',1X,'A64',1X,'A66',1X,'A68',1X,'A70',1X,'A72',1X,'A74',1X,'A76',1X,'A78',1X,'A80',1X,'A82',1X,'A84',1X,'A86',1X,'A88',1X,'A90',1X,'A92',1X,'A94',1X,'A96',1X,'A98',1X,'A100')
955  FORMAT(11X,'A2',1X,'A4',1X,'A6',1X,'A8',1X,'A10',1X,'A12',1X,'A14',1X,'A16',1X,'A18',1X,'A20',1X,'A22',1X,'A24',1X,'A26',1X,'A28',1X,'A30',1X,'A32',1X,'A34',1X,'A36',1X,'A38',1X,'A40',1X,'A42',1X,'A44',1X,'A46',1X,'A48',1X,'A50',1X,'A52',1X,'A54',1X,'A56',1X,'A58',1X,'A60',1X,'A62',1X,'A64',1X,'A66',1X,'A68',1X,'A70',1X,'A72',1X,'A74',1X,'A76',1X,'A78',1X,'A80',1X,'A82',1X,'A84',1X,'A86',1X,'A88',1X,'A90',1X,'A92',1X,'A94',1X,'A96',1X,'A98',1X,'A100')
956  FORMAT(4E16.9)
957  FORMAT(4E16.9)
999  STOP
    END
0021023013 IS THE LOCATION FOR EXCEPTIONAL ACTION ON THE I/O STATEMENT AT 00210030
0021023015 IS THE LOCATION FOR EXCEPTIONAL ACTION ON THE I/O STATEMENT AT 00210035
0021023011 IS THE LOCATION FOR EXCEPTIONAL ACTION ON THE I/O STATEMENT AT 00210040
0021023013 IS THE LOCATION FOR EXCEPTIONAL ACTION ON THE I/O STATEMENT AT 00210045
0021023015 IS THE LOCATION FOR EXCEPTIONAL ACTION ON THE I/O STATEMENT AT 00210030
0021023011 IS THE LOCATION FOR EXCEPTIONAL ACTION ON THE I/O STATEMENT AT 00210035
0021023013 IS THE LOCATION FOR EXCEPTIONAL ACTION ON THE I/O STATEMENT AT 00210030
    SEGMENT 002 IS 0288 LONG

```



SSURKOUTINE IMPULS(MCONVL,NPATM,U2,0300)

D-7



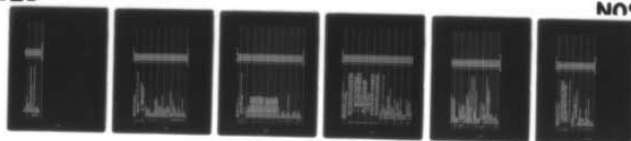
AD-A054 726

SYSTEMS EXPLORATION INC SAN DIEGO CA  
HF CHANNEL SIMULATOR FOR WIDEBAND SIGNALS. A  
MAR 78 R LUGANNANI, H C BOOKER, L E HOFF  
NOSC-TR-208

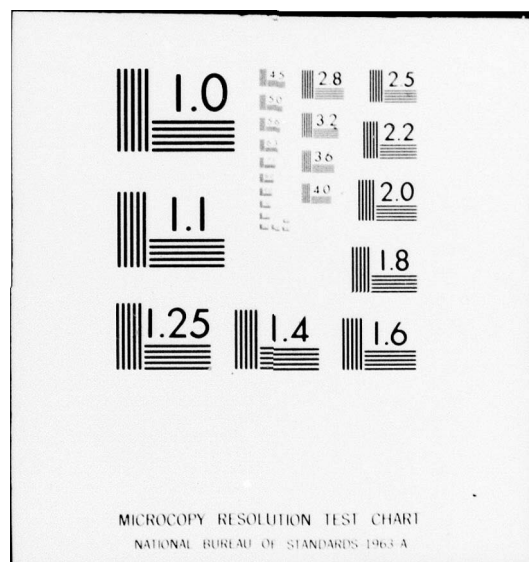
F/G 17/2  
MATHEMATICAL MODEL--ETC(U)  
N00123-76-C-1090  
AH

UNCLASSIFIED

2 OF 2  
AD  
A054726



END  
DATE  
FILMED  
7-78  
DDC



K1=N-1	C	0091008210
K2=N-2	C	0091008312
K1=(FLOAT(K1/2)+1.E-06	C	0091008415
XIND=N-ZNT	C	0091008715
XINDC=1-XIND	C	0091008914
XI(K)=(1/(2.5002))*(2.51+CEXP(-A1*02))*(XINDC-COS(ARG)*A1*XINDC	C	0091008A15
1/(ARG))*ARG*X1(K1)-A1*FLOAT(K1)*X1(K2)	C	0091008B12
CONTINUE	C	0091008C10
45 D1(K2)=5*(X10-A1*003)*X1(K1)-15*(003*02)*X1(K1)*A1*(1./A1)*(003*02)*	C	0091008D11
X1(K2))	C	0091008E13
50 CONTINUE	C	0091008F15
100 CONTINUE	C	0091008G10
RETURN	C	0091008H11
END	C	0091008I14
SEGMENT 009 IS ODD LONG		

	SUBROUTINE FRESNEL(D2,ARG,XIO) COMPLEX A1,C2,C3,CS,HN,HS,XIO		START OF SEGMENT UOC
C			C 00C1000010
C	SUBROUTINE COMPUTES COMPLEX FRESNEL INTEGRAL USING RATIONAL APPROXIMATION.		C 00C1000010
C			C 00C1000010
C	D2 = AMPLITUDE DISTORTION COEFFICIENT		C 00C1000010
C	ARG = ARGUMENT OF FRESNEL INTEGRAL		C 00C1000010
C	XIO = COMPLEX FRESNEL INTEGRAL		C 00C1000010
	PI=3.14159265359		C 00C1000010
	A1=0.01		C 00C1000010
	ARG=ABS(ARG)		C 00C1000010
	IF(C2)1,35,2		C 00C1000010
1	SUM=1.		C 00C1000010
	GOTO3		C 00C1000010
2	SUM=1.		C 00C1000010
3	D2=ABS(C2)		C 00C1000010
	SUM=ABS(1+((ARG/(2+D2)))		C 00C1000010
	DIF=ABS(1-((ARG/(2+D2)))		C 00C1000010
	C1=SQRT(PI/(2+D2))		C 00C1000010
	C2=EXP(-A1*D2)		C 00C1000010
	C3=CFAP(A1*ARG)		C 00C1000010
	C4=EXP(-A1*ARG)		C 00C1000010
	C5=EXP(C1*(ARG+2337/(2+D2)))		C 00C1000010
	ASUM=SUM/C1		C 00C1000010
	AUIF=DIF/C1		C 00C1000010
	W=ARG-2+D2		C 00C1000010
	CALL HCDIFF(HU)		C 00C1000010
	CALL H(CASUM,HS)		C 00C1000010
	IF(W>10,10		C 00C1000010
5	XIO=(C1-A1)*C1+CS-C1+C2*(HN+C3+HS+C4)		C 00C1000010
	GOTO20		C 00C1000010
10	XIO=C1+C2*(HN+C3+HS+C4)		C 00C1000010
20	IF(SCN7525530		C 00C1000010
25	XIO=CONJG(XIO)		C 00C1000010
30	CONTINUE		C 00C1000010
	GOTO40		C 00C1000010
35	IF(ARG)37,36,37		C 00C1000010
36	XIO=(2+D2)		C 00C1000010
	GOTO40		C 00C1000010
37	XIO=((2+D2)*SIN(ARG))/ARG		C 00C1000010
40	CONTINUE		C 00C1000010
	RETURN		C 00C1000010
	END		C 00C1000010
		SEGMENT UOC IS UO0A LUNG	



D-10

D-11





SEGMENT 013 IS 0029 LUNG



M  
-C